the expression of a series of IFN-responsive genes were observed at the later stages (48 hr) of differentiation. We speculate that the feedback loop may regulate the early phase of differentiation and that, once the cells pass through that phase, they may become resistant to IFN in terms of the osteoclastogenesis. In support, fos has been shown to be replaced by known downstream effectors, including Fra1 and Fra2 (Table 2) in the later phase of osteoclast differentiation (40). The regulation and relationship between IFN and fos family proteins are interesting issues worth further study.

In addition, several genes for lysosomal enzymes and the lysosomal marker, LAMP2, were shown to be down-regulated. Active osteoclasts are highly polarized and possess bone-resorbing activity by providing acidified compartments and hydrolyzing enzymes, including MMP9 and cathepsin K, between the apical surface and sealing zones of osteoclasts and the bone surface. It has been reported that the resorption compartment is similar to early endosomes and lysosomes (41,42). The decrease in the expression of the lysosomal genes throughout osteoclast differentiation that were shown in our study may support the idea that the ruffled border membrane and the acidified extracellular compartment are specialized for bone matrix resorption and different from the lysosomes observed in other cell types.

We also identify a gene encoding ZNF216 as up-regulated by RANKL-induced osteoclast differentiation. Furthermore, ectopic expression of full-length ZNF216 inhibited but the zinc finger-truncated mutants accelerated osteoclast differentiation. Because the gene was also up-regulated by TNFα, RANKL may share common machinery with TNFα in induction of ZNF216 expression. Factors known to activate NF-κB, such as LPS and TPA, also up-regulated the expression of ZNF216. It is of interest that the promoter region of human ZNF216 gene contains a possible NF-κB response element (data not shown). These results suggested that a probable factor involved in the induction of ZNF216 is the NF-κB transcription factor, although further experiments are required. In support, IFNβ is a strong negative regulator of osteoclastogenesis (43,44), and expression of ZNF216 suppressed osteoclast differentiation in our study. Therefore, ZNF216 may take part in the IFN-mediated regulatory mechanism NF-κB.

The precise molecular function of ZNF216 is still unclear. It has been reported that ZNF216 may inhibit the NF-κB pathway (29). Although we have examined the influence of ZNF216 on NF-κB activation, neither inhibition of nuclear translocation nor DNA-binding ability of NF-κB was reproduced by ectopic expression of full-length or truncated mutants of ZNF216 (not shown). Furthermore, we have tested the NF-κB inhibitory activity of ZNF216, as well as A20 protein, using reporter gene constructs. Ectopic expression of A20, but not full-length ZNF216, strongly inhibited NF-κB activation (data not shown). In addition, no endogenous NEMO or RIP protein was detected in a proteome analysis of the ZNF216 complex (unpublished observation). Therefore, ZNF216

does not seem to be a direct regulator of the NF-κB signaling pathway, although its involvement is still under investigation. It was recently described that one of the seven A20-type zinc finger domains in A20 protein possesses E3 ubiquitin ligase activity (45). Thus, ZNF216 also may be involved in ubiquitin-related systems. It is of interest that our expression studies resulted in opposing phenotypes in osteoclastogenesis that were largely dependent on the mutation. Thus, the truncated mutants may act in a dominant negative manner compared with the endogenous or wild-type ZNF216. How does ZNF216 inhibit osteoclastogenesis without affecting NF-κB pathway? Future studies will be aimed at elucidation of the molecular mechanisms involved in ZNF216-mediated osteoclast differentiation.

ACKNOWLEDGMENT

The authors dedicate this paper to our colleague, Dr. Katsunori Mizuno, who passed in December 2004. We are grateful to Drs. Kunihiro Matsumoto and Naoki Sakurai for providing RANK293 cells; Dr. Koichi Matsuo for helpful discussions; and John Grzesiak for proofreading the manuscript. This work is supported in part by a grant from the Program for Promotion of Fundamental Studies in Health Sciences of the Organization for Pharmaceutical Safety and Research of Japan, and by a Research Grant for Longevity Sciences from the Ministry of Health, Labor and Welfare.

REFERENCES

1. Ash P, Loutit JF, Townsend KM. Osteoclasts derived from haematopoietic stem cells. Nature **1980**, *283*, 669–670.

2. Suda T, Udagawa N, Takahashi N. Osteoclast generation. In: (Bilezikian JP, Raisz LG, Rodan CA, Eds. *Principles of Bone Biology*. San Diego: Academic Press, 1996, 87–102.

3. Roodman GD. Advances in bone biology: The osteoclast. Endocr Rev **1996**, 17; 308–332.

4. Yoshida H, Hayashi S, Kunisada T, Ogawa M, Nishikawa S, Okamura H, Sudo T, Shultz LD, Nishikawa S. The murine mutation osteopetrosis is in the coding region of the macrophage colony stimulating factor gene Nature **1990**, *345*, 442–444.

5. Pfeilschifter J, Chenu C, Bird A, Mundy GR, Roodman GD. Interleukin-1 and tumor necrosis factor stimulate the formation of human osteoclast-like cells in vitro. J Bone Miner Res **1989**, *4*, 113–118.

6. Kobayashi K, Takahashi N, Jimi E, Udagawa N, Takami M, Kotake S, Nakagawa N, Kinosaki M, Yamaguchi K, Shima N, Yasuda H, Morinaga T, Higashio K, Martin TJ, Suda T. Tumor necrosis factor alpha stimulates osteoclast differentiation by a mechanism independent of the ODF/RANKL-RANK interaction. J Exp Med **2000**, *191*, 275–286.

7. Lacey DL, Timms E, Tan H-L, Kelley MJ, Dunstan CR, Burgess T, Elliott R, Colombero A, Elliott G, Scully S, Hsu H, Sullivan J, Hawkins N, Davy E, Capparelli C, Eli A, Qian Y-X, Kaufman S, Sarosi I, Shalhoub V, Senaldi G, Guo J, Delaney J, Boyle

WJ. Osteoprotegerin ligand is a cytokine that regulates osteoclast differentiation and activation. Cell **1998**, *93*, 165–176

8. Yasuda H, Shima N, Nakagawa N, Yamaguchi K, Kinosaki M, Mochizuki S, Tomoyasu A, Yano K, Goto M, Murakami A, Tsuda E, Morinaga T, Higashio K, Udagawa N, Takahashi N, Suda T. Osteoclast differentiation factor is a ligand for osteoprotegerin/osteoclastogenesis-inhibitory factor and is identical to TRANCE/RANKL. Proc Natl Acad Sci USA **1998**, *95*, 3597–3602.

9. Kong Y-Y, Yoshida H, Sarosi I, Tan H-L, Timms E, Capparelli C, Morony S, Oliveira-dos-Santos AJ, Van G, Itie A, Khoo W, Wakeham A, Dunstan CR, Lacey DL, Mak TW, Boyle WJ, Penninger JM. OPGL is a key regulator of osteoclastogenesis, lymphocyte development and lymph-node organogenesis. Nature **1999**, *397*, 315–323

10. Li J, Sarosi I, Yan X-Q, Morony S, Capparelli C, Tan H-L, McCabe S, Elliott R, Scully S, Van G, Kaufman S, Juan S-C, Sun Y, Tarpley J, Martin L, Christensen K, McCabe J, Kostenuik P, Hsu H, Fletcher F, Dunstan CR, Lacey DL, Boyle WJ. RANK is the intrinsic hematopoietic cell surface receptor that controls osteoclastogenesis and regulation of bone mass and calcium metabolism. Proc Natl Acad Sci USA **2000**, *97*, 1566–1571.

11. Fuller K, Wong B, Fox S, Choi Y, Chambers TJ. TRANCE is necessary and sufficient for osteoblast-mediated activation of bone resorption in osteoclasts. J Exp Med **1998**, *188*, 997–1001.

12. Lotsova V, Caamano J, Loy J, Yang Y, Lewin A, Bravo R. Osteopetrosis in mice lacking NF-κB1 and NF-κB2. Nat Med **1997**, *3*, 1285–1289.

13. Grigoriadis AE, Wang ZQ, Cecchini MG, Hofstetter W, Felix R, Fleisch HA, Wagner EF. c-Fos: A key regulator of osteoclast-macrophage lineage determination and bone remodeling. Science **1994**, *266*, 443–448.

14. Wagner EF, Matsuo K. Signalling in osteoclasts and the role of Fos/AP1 proteins. Ann Rheum Dis **2003**, *62*, 83–85.

15. Soriano P, Montgomery C, Geske R, Bradley A. Targeted disruption of the c-src proto-oncogene leads to osteopetrosis in mice. Cell **1991**, *64*, 693–702.

16. Boyce BF, Yoneda T, Lowe C, Soriano P, Mundy GR. Requirement of pp60c-src expression for osteoclasts to form ruffled borders and resorb bone in mice. J Clin Invest **1992**, *90*, 1622–1627.

17. Tanaka S, Takahashi N, Udagawa N, Sasaki T, Fukui Y, Kurokawa T, Suda T. Osteoclasts express high levels of p60c-src, preferentially on ruffled border membranes. FEBS Lett **1992**, *313*, 85–89.

18. Mizukami J, Takaesu G, Akatsuka H, Sakurai H, Ninomiya-Tsuji J, Matsumoto K, Sakurai N. Receptor activator of NF-kappaB ligand (RANKL) activates TAK1 mitogen-activated protein kinase kinase kinase through a signaling complex containing RANK, TAB2, and TRAF6. Mol Cell Biol **2002**, *22*, 992–1000.

19. Yousef, AA. IL-4 abrogates osteoclastogenesis through STAT6-dependent inhibition of NF-κ B J Clin Invest **2001**, *107*, 1375–1385.

20. Battaglino R, Kim D, Fu J, Vaage B, Fu XY, Stashenko P. c-myc is required for osteoclast differentiation. J Bone Miner Res **2002**, *17*, 763–773.

21. Matsuo K, Galson DL, Zhao C, Peng L, Laplace C, Wang KZ, Bachler MA, Amano H, Aburatani H, Ishikawa H, Wagner EF. Nuclear factor of activated T-cells (NFAT) rescues osteoclastogenesis in precursors lacking c-Fos. J Biol Chem **2004**, *279*, 26475–26480.

22. Takayanagi H, Ogasawara K, Hida S, Chiba T, Murata S, Sato K, Takaoka A, Yokochi T, Oda H, Tanaka K, Nakamura K, Taniguchi T. T-cell-mediated regulation of

osteoclastogenesis by signalling cross-talk between RANKL and IFNγ. Nature **2000**, *408*, 600–605.

23. Scott DA, Greinwald JH, Jr, Marietta JR, Drury S, Swiderski RE, Vinas A, DeAngelis MM, Carmi R, Ramesh A, Kraft ML, Elbedour K, Skworak AB, Friedman RA, Srikumari Srisailapathy CR, Verhoeven K, Van Gamp G, Lovett M, Deininger PL, Batzer MA, Morton CC, Keats BJ, Smith RJ, Sheffield VC. Identification and mutation analysis of a cochlear-expressed, zinc finger protein gene at the DFNB7/11 and dn hearing-loss loci on human chromosome 9q and mouse chromosome 19. Gene **1998** *215*, 461–469.

24. Hofbauer LC, Khosla S, Dunstan CR, Lacey DL, Boyle WJ, Riggs BL. The roles of osteoprotegerin and osteoprotegerin ligand in the paracrine regulation of bone resorption. J Bone Miner Res **2000**, *15*, 2–12.

25. Castagna M, Takai Y, Kaibuchi K, Sano K, Kikkawa U, Nishizuka Y. Direct activation of calcium-activated, phospholipid-dependent protein kinase by tumor-promoting phorbol esters. J Biol Chem, **1982** *257*, 7847–7851.

26. Hirano M, Hirai S, Mizuno K, Osada S, Hosaka M, Ohno S. A protein kinase C isoenzyme, nPKCε, is involved in the activation of NF-κB by 12-O-tetradecanoylphorbol-13-acetate (TPA) in rat 3Y1 fibroblasts. Biochem Biophys Res Commun **1995**, *206*, 429–436.

27. Chen Y, Wu Q, Song S-Y, Su W-J. Activation of JNK by TPA promotes apoptosis via PKC pathway in gastric cancer cells. World J. Gastroenterol **2002**, *8*, 1014–1018.

28. Linnen JM, Bailey CP, Weeks D. L. Two related localized mRNAs from Xenopus laevis encode ubiquitin-like fusion proteins. Gene **1993**, *128*, 181–188

29. Huang J, Teng L, Li L, Liu T, Li L, Chen D, Xu LG, Zhai Z, Shu HB. ZNF216 is an A20-like and IκB kinase γ-interacting inhibitor of NFκB activation. J Biol Chem **2004**, *279*, 16847–16853.

30. Whiteside ST, Israel A. IκB proteins: Structure, function and regulation. Semin Cancer Biol **1997**, *8*, 75–82.

31. Kaifu T, Nakahara J, Inui M, Mishima K, Momiyama T, Kaji M, Sugahara A, Koito H, Ujike-Asai A, Nakamura A, Kanazawa K, Tan-Takeuchi K, Iwasaki K, Yokoyama WM, Kudo A, Fujiwara M, Asou H, Takai T. Osteopetrosis and thalamic hypomyelinosis with synaptic degeneration in DAP12-deficient mice. J Clin Invest **2003**, *111*, 323–332.

32. Koga T, Inui M, Inoue K, Kim S, Suematsu A, Kobayashi E, Iwata T, Ohnishi H, Matozaki T, Kodama T, Taniguchi T, Takayanagi H, Takai T. Costimulatory signals mediated by the ITAM motif cooperate with RANKL for bone homeostasis. Nature **2004**, *428*, 758–763.

33. Mocsai A, Humphrey MB, Van Ziffle JA, Hu Y, Burghardt A, Spusta SC, Majumdar S, Lanier LL, Lowell CA, Nakamura MC. The immunomodulatory adapter proteins DAP12 and Fc receptor gamma-chain (FcRgamma) regulate development of functional osteoclasts through the Syk tyrosine kinase. Proc Natl Acad Sci USA **2004**, *101*, 6158–6163.

34. Daeron M. Fc receptor biology. Annu Rev Immunol **1997**, *15*, 203–234.

35. Nakajima H, Samaridis J, Angman L, Colonna M. Human myeloid cells express an activating ILT receptor (ILT1) that associates with Fc receptor gamma-chain. J Immunol **1999**, *162*, 5–8.

36. Cella M, Buonsanti C, Strader C, Kondo T, Salmaggi A, Colonna M. Impaired differentiation of osteoclasts in TREM-2-deficient individuals. J Exp Med **2003**, *198*, 645–651.

37. Paloneva J, Mandelin J, Kiialainen A, Bohling T, Prudlo J, Hakola P, Haltia M, Konttinen YT, Peltonen L. DAP12/TREM2 deficiency results in impaired osteoclast differentiation and osteoporotic features. J Exp Med **2003**, *198*, 669–675.

38. Takayanagi H, Kim S, Taniguchi T. Signaling crosstalk between RANKL and interferons in osteoclast differentiation. Arthritis Res **2002a**, *4*, S227–S232.

39. Takayanagi H, Kim S, Matsuo K, Suzuki H, Suzuki T, Sato K, Yokochi T, Oda H, Nakamura K, Ida N, Wagner EF, Taniguchi T. RANKL maintains bone homeostasis through c-Fos-dependent induction of interferon-beta. Nature **2002b**, *416*, 744–749.

40. Matsuo K, Owens JM, Tonko M, Elliott C, Chambers TJ, Wagner EF. Fosl1 is a transcriptional target of c-Fos during osteoclast differentiation Nat Genet **2000**, *24*, 184–187.

41. Palokangas H, Mulari M, Vaananen HK. Endocytic pathway from the basal plasma membrane to the ruffled border membrane in bone-resorbing osteoclasts. J Cell Sci **1997**, *110*, 1767–1780.

42. Stenbeck G. Formation and function of the ruffled border in osteoclasts. Semin Cell Dev Biol **2002**, *13*, 285–292.

43. Gowen M, Mundy GR. Actions of recombinant interleukin 1, interleukin 2, and interferon-gamma on bone resorption in vitro. J Immunol **1986**, *136*, 2478–2482.

44. Takahashi N, Mundy GR, Roodman GD. Recombinant human interferon-gamma inhibits formation of human osteoclast-like cells. J Immunol **1986**, *137*, 3544–3549.

45. Wertz IE, O'Rourke KM, Zhou H, Eby M, Aravind L, Seshagiri S, Wu P, Wiesmann C, Baker R, Boone DL, Ma A, Koonin EV, Dixit VM. De-ubiquitination and ubiquitin ligase domains of A20 downregulate NF-kappaB signalling. **2004**, *430*, 694–699.

The EMBO Journal (2006) 25, 554–564 | © 2006 European Molecular Biology Organization | All Rights Reserved 0261-4189/06
www.embojournal.org

THE EMBO JOURNAL

A novel ubiquitin-binding protein ZNF216 functioning in muscle atrophy

Akinori Hishiya[1,2], Shun-ichiro Iemura[3], Tohru Natsume[3], Shinichi Takayama[2], Kyoji Ikeda[1] and Ken Watanabe[1,*]

[1]Department of Bone & Joint Disease, National Center for Geriatrics & Gerontology (NCGG), Obu, Aichi, Japan, [2]Program of Molecular Chaperone Biology, Department of Radiology, Medical College of Georgia, Augusta, GA, USA and [3]Japan Biological Information Research Center (JBIRC), National Institute of Advanced Industrial Science & Technology (AIST), Tokyo, Japan

The ubiquitin–proteasome system (UPS) is critical for specific degradation of cellular proteins and plays a pivotal role on protein breakdown in muscle atrophy. Here, we show that ZNF216 directly binds polyubiquitin chains through its N-terminal A20-type zinc-finger domain and associates with the 26S proteasome. ZNF216 was colocalized with the aggresome, which contains ubiquitinylated proteins and other UPS components. Expression of *Znf216* was increased in both denervation- and fasting-induced muscle atrophy and upregulated by expression of constitutively active FOXO, a master regulator of muscle atrophy. Mice deficient in *Znf216* exhibited resistance to denervation-induced atrophy, and ubiquitinylated proteins markedly accumulated in neurectomized muscle compared to wild-type mice. These data suggest that ZNF216 functions in protein degradation via the UPS and plays a crucial role in muscle atrophy.

The EMBO Journal (2006) **25,** 554–564. doi:10.1038/sj.emboj.7600945; Published online 19 January 2006
Subject Categories: proteins; molecular biology of disease
Keywords: aggresome; muscular atrophy; proteasome; ubiquitin; zinc-finger protein

Introduction

The ubiquitin–proteasome system (UPS) is one of the major protein degradation pathways in eukaryotic cells. The UPS plays key regulatory roles in many cellular processes, including cell cycle control, the regulation of transcription and protein quality control (Hershko and Ciechanover, 1998; Pickart and Cohen, 2004). Aberrations of this system lead to many forms of pathogenesis, such as malignancies, neurodegenerative disease and inflammatory response (Glickman and Ciechanover, 2002). The UPS includes sequential, multistep reactions: ubiquitin-conjugation of target proteins by E1, E2 and E3 enzymes, recognition of ubiquitinylated proteins by ubiquitin-binding proteins or 19S subunits of proteasome and proteolysis in the proteasome.

Many catabolic conditions, such as low-insulin state, hyperthyroidism, sepsis and cancer cachexia lead to enhancement of protein breakdown in skeletal muscle known as muscle atrophy (Mitch and Goldberg, 1996; Lecker *et al*, 1999). In muscle atrophy, the UPS plays a pivotal role in protein breakdown (Price *et al*, 1996; Tawa *et al*, 1997). Several studies indicate that mRNAs encoding UPS components are increased in atrophying muscle (Medina *et al*, 1991; Wing and Goldberg, 1993; Bailey *et al*, 1996; Price *et al*, 1996; Jagoe *et al*, 2002). In particular, the E3 ubiquitin ligases MAFbx/Atrogin-1 and MuRF-1 (muscle RING finger 1) are known to be markers of muscle atrophy (Bodine *et al*, 2001; Gomes *et al*, 2001). Both are induced in multiple models of muscle atrophy including immobilization, denervation and hindlimb suspension, and mice deficient in either gene are resistant to denervation-induced muscle atrophy (Bodine *et al*, 2001). Goldberg and co-workers proposed that atrophy-related genes, whose expression is induced in multiple types of muscle atrophy, are called 'atrogenes' (Sandri *et al*, 2004). Recently, it was demonstrated that the IGF-I/PI3K/Akt pathway is an important regulator of muscle mass in muscle hypertrophy and atrophy (Sacheck *et al*, 2004; Sandri *et al*, 2004; Stitt *et al*, 2004). In that case, the transcription factor FOXO plays a pivotal role in activating atrogenes such as MAFbx/Atrogin-1 (Gomes *et al*, 2001).

Although many UPS players such as E3 ligases have been characterized, the mechanism of how ubiquitinylated proteins are delivered to the proteasome have not been fully elucidated. A component of 19S proteasome, Rpn10/S5a, recognizes the ubiquitinylated proteins (Young *et al*, 1998; Wilkinson *et al*, 2000). It has been shown that yeast proteins, Rad23p and Dsk2p, bind to ubiquitinylated substrates and to the 26S proteasome through their UBA and Ubl domains, respectively, thereby functioning as shuttle proteins that present polyubiquitinylated proteins to the proteasome (Chen *et al*, 2001; Funakoshi *et al*, 2002; Elsasser and Finley, 2005). Loss-of-function of shuttle proteins results in abnormal accumulation of polyubiquitinylated proteins (Lambertson *et al*, 1999; Saeki *et al*, 2002). However, yeast can survive when both *RAD23* and *DSK2* genes are mutated, suggesting that other mechanisms or molecule(s) possessing a shuttle function exist (Saeki *et al*, 2002). Here, we show that ZNF216, a novel ubiquitin-binding protein containing an A20-type zinc-finger, is such a factor. *Znf216* expression is upregulated in skeletal muscle in experimental models of muscle atrophy, and *Znf216*-deficient mice exhibit resistance to muscle atrophy accompanied by abnormal accumulation of polyubiquitinylated proteins in skeletal muscle. Our findings suggest that ZNF216, with its potential function of anchoring ubiquitinylated proteins to the proteasome, plays a critical role in degrading muscle proteins.

*Corresponding author. Department of Bone & Joint Disease, National Center for Geriatrics & Gerontology (NCGG), Obu, Aichi 474-8522, Japan. Tel.: +81 562 46 2311; Fax: +81 562 44 6595;
E-mail: kwatanab@nils.go.jp

Received: 6 June 2005; accepted: 14 December 2005; published online: 19 January 2006

Results

ZNF216 directly binds to polyubiquitin

We have identified a gene, *Znf216* (*Za20d2*, Mouse Genome Informatics), encoding an A20 zinc-finger (Znf-A20) motif-containing protein, as a RANKL-induced gene upregulated upon osteoclast formation using a microarray technique (Hishiya *et al*, 2005). *Znf216* was originally identified as a candidate gene for hearing loss and is expressed in cochlear and skeletal muscle (Scott *et al*, 1998; Huang *et al*, 2004). To determine the function of ZNF216, we searched for molecules that associate with ZNF216 using yeast two-hybrid screening and isolated several clones encoding a gene for polyubiquitin C. To determine whether ZNF216 interacts with ubiquitin in mammalian cells, we transfected HEK293 cells with an expression vector for FLAG-tagged ZNF216 and HA-tagged ubiquitin and performed co-immunoprecipitation experiments. ZNF216 possesses A20-type (amino acids 11–35) and AN1-type (amino acids 154–191) zinc-finger domains at its N- and C-termini, respectively (Figure 1A). Endogenous ubiquitinylated proteins, which appear as smears, were co-immunoprecipitated with FLAG-tagged ZNF216 (Figure 1B). Notably, N-terminal deletion (ΔN; amino acids 36–213) or point mutants (M1 and M3) of the A20-type zinc-finger (ZnF-A20) domain abolished ubiquitin-binding ability of ZNF216, indicating that the ZnF-A20 domain is indispensable for binding to ubiquitin (Figures 1A and B). Whereas in non-denaturing conditions, ubiquitinylated molecules were present with FLAG-tagged ZNF216, these molecules completely disappear from immunoprecipitates following heat denaturation, which abolishes noncovalent protein–protein interactions (Figure 1C), suggesting that ZNF216 associates with ubiquitinylated proteins rather than being ubiquitinylated itself. Next, to determine whether ZNF216 binds to ubiquitin directly, we performed GST pull-down assays using GST-ZNF216 fusion proteins (Figure 1D) and purified polyubiquitin. As shown in Figure 1E, GST-ZNF216 but not GST bound to polyubiquitin chains. As expected, binding of ZNF216 to polyubiquitin chains was completely abolished by a point mutation in the ZnF-A20 domain (M1, Figure 1E). Furthermore, a GST fusion protein containing only the ZnF-A20 domain (amino acids 2–60) could bind to polyubiquitin chains, suggesting that ZNF216 directly binds to polyubiquitin chains, and that the ZnF-A20 domain is required for binding to polyubiquitin. As for other ZnF-A20 containing proteins, AWP1 (ZA20D3) also possessed polyubiquitin-binding activity but the ZnF-A20 domain(s) of Rabex-5 (Horiuchi *et al*, 1997) and A20/TNFAIP3 (Opipari *et al*, 1990) proteins did not (Supplementary Figure S1).

ZNF216 associates with the 26S proteasome

We also identified molecules associating with ZNF216 by proteomic analysis of complexes formed with FLAG-tagged ZNF216. Molecules expressed in HEK293 cells and that co-immunoprecipitated with FLAG-tagged ZNF216 were analyzed by tandem mass spectrometry. By this analysis, every subunit of the 26S proteasome complex was identified as associating with FLAG-tagged ZNF216 (data not shown). To identify the region of ZNF216 required for association with the 26S proteasome, lysates of cells expressing either FLAG-tagged ZNF216 or its mutants were immunoprecipitated with anti-FLAG antibody. Co-precipitation of proteasomal components was monitored by immunoblotting using an antibody against Rpn7p (S10a), a non-ATPase subunit of the 19S regulatory subunit. As shown in Figure 2A, this protein efficiently co-precipitated with FLAG-tagged ZNF216. The interaction was also observed with truncated or point mutants of ZnF-A20 (ΔN or M1), indicating that ubiquitin-binding ability is dispensable for association with the 26S proteasome. To determine whether endogenous ZNF216 proteins are also associated with the 26S proteasome, we performed a GST pull-down assay using the ubiquitin-like (Ubl) domain of hHR23B, a human homologue of Rad23, which is known to bind to the 26S proteasome. As shown in Figure 2B, GST-Ubl but not GST was pulled down with the endogenous 26S proteasome. Endogenous ZNF216 was also detected in the GST-Ubl/26S proteasome complex (upper panels, Figure 2B). Furthermore, purified recombinant ZNF216 did not bind to GST-Ubl (lower panel, Figure 2B), suggesting that endogenous ZNF216 is not directly bound to the Ubl domain but associates with the 26S proteasome.

Colocalization with the aggresome

Next, we determined the subcellular localization of ZNF216. Indirect immunofluorescence of ZNF216 expressed in COS-7 cells showed that the protein was largely cytoplasmic but was seen to a lesser extent in the nucleus (Figure 3A). Aggresomes, which are insoluble aggregates of ubiquitinylated proteins complexed with the proteasome and induced by treatment with proteasome inhibitors, are known to mimic inclusions seen in pathogenic UPS disorders (Johnston *et al*, 1998; Kopito, 2000; Lelouard *et al*, 2002). As shown in Figures 3D–H, ZNF216 proteins were colocalized with aggresomes induced by treatment with the proteasome inhibitor MG132. ZNF216 itself was not ubiquitinylated as shown in Figure 1C.

Induction of ZNF216 expression upon muscle atrophy

Biochemical and cell biological evidence presented here strongly suggests that ZNF216 functions in the UPS. In skeletal muscle, it is generally accepted that the UPS plays a critical role in muscular atrophy, and expression of atrophy-related genes including those encoding UPS components is induced in atrophying muscle (Jagoe *et al*, 2002; Lecker *et al*, 2004). As *Znf216* was predominantly expressed in brain and skeletal muscle (Scott *et al*, 1998), we investigated the relationship between ZNF216 and muscle atrophy. To determine whether *Znf216* expression is induced during muscle atrophy, an *in vitro* model of muscle atrophy was utilized. It has been reported that addition of dexamethasone to cultures of differentiated C2C12 myotubes causes formation of myotubes exhibiting signs of atrophy, including a reduction in myotube diameter (Stitt *et al*, 2004). Such treatment dramatically induced expression of *Znf216* (Figure 4A).

Next, expression of *Znf216* was determined in *in vivo* experimental models of muscle atrophy. Mice that undergo fasting for 2 days show significant decreases in body weight, as well as in the mass of the gastrocnemius muscles (data not shown). In this model, fasting for 2 days results in dramatic increases in *Znf216* mRNA (Figure 4B) and protein (Supplementary Figure S3) in muscle. Although there were differences in induction patterns of two differently sized transcripts of Znf216 by atrophy-inducting stimuli, both transcripts encode the same protein (Supplementary Figures

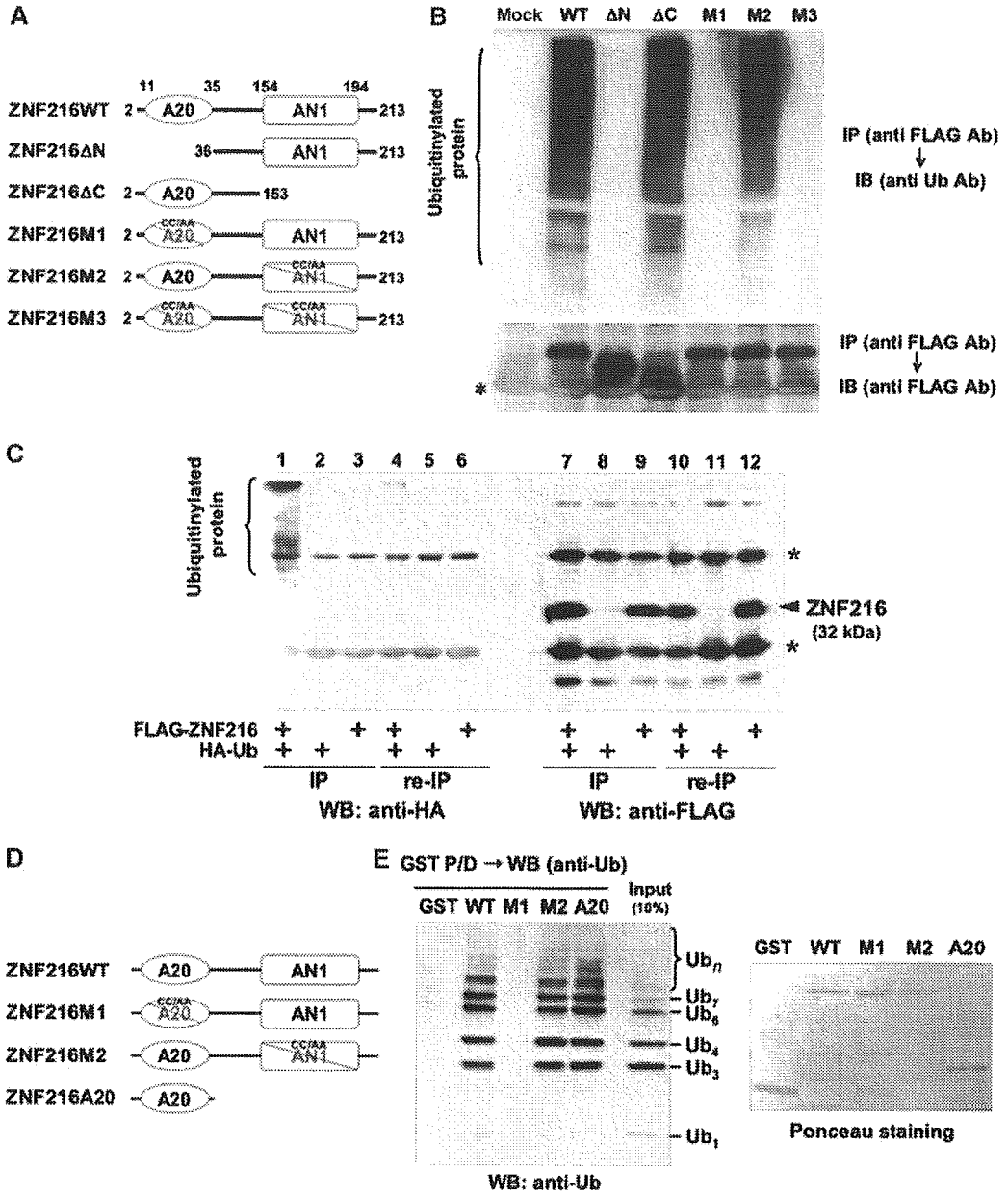

Figure 1 ZNF216 binds polyubiquitin directly through the ZnF-A20 domain. (**A**) Schematic representation of the primary structure of wild-type ZNF216 and its mutants. ZNF216ΔN (aa 36–213) and ZNF216ΔC (aa 2–153) constructs lack the ZnF-A20 (aa 11–35) and ZnF-AN1 (aa 154–194) domains, respectively. Cysteine residues at positions 30 and 33 within the ZnF-A20 were substituted with alanines (C30A/C33A) in ZNF216M1, and both cysteines 170 and 175 within the ZnF-AN1 were substituted with alanines (C170A/C175A) in ZNF216M2. Both ZnF-A20 and ZnF-AN1 domains were mutated in ZNF216M3. (**B**) Co-precipitation of ubiquitinylated proteins and ZNF216. FLAG-tagged ZNF216 or mutants were expressed in HEK293 cells, and cell extracts were immunoprecipitated with anti-FLAG antibody. Ubiquitinylated proteins detected with anti-ubiquitin antibody were precipitated with FLAG-tagged ZNF216 but not with ZnF-A20 mutants. Expression levels of FLAG-tagged ZNF216 constructs are shown at the bottom. Bands corresponding to immunoglobulin chains are marked by an asterisk. (**C**) ZNF216 is minimally ubiquitinylated. HEK293 cells expressing FLAG-tagged ZNF216 or HA-tagged ubiquitin were lysed and immunoprecipitation was performed using anti-FLAG antibody. Aliquots of precipitated beads were boiled and immunoprecipitated again (re-IP). Each sample was separated on gels and probed with anti-HA (left) or anti-FLAG antibody (right). Bands for immunoglobulin chains are marked by asterisks. (**D**) Constructs used for *in vitro* binding assay. ZNF216WT, ZNF216M1 and ZNF216 M2 were as indicated in (A). ZNF216A20 possesses only the A20 domain (aa 2–60). All constructs were produced as GST fusion proteins. (**E**) *In vitro* ubiquitin binding assay. Left panel: GST protein fused to the constructs indicated in (D) was incubated with purified K48-linked polyubiquitin chains, followed by precipitation with GSH beads. In all, 10% of purified polyubiquitin chains was separated without pull-down to evaluate protein amount (10% input). Right panel: the membrane was stained with ponceau to evaluate levels of GST fusion protein.

S2 and S3). Expression of MuRF-1 (Figure 4B) and MAFbx (Gomes *et al*, 2001) was also induced in fasting. Upregulation of *Znf216* was also observed in a model of denervation-induced muscle atrophy. Neurectomy promotes significant reduction (~20%) in the weight of gastrocnemius muscles within the first 7 days postsurgery. As expected, expression of *Znf216* and MuRF-1 was induced in gastrocnemius muscles by denervation-induced muscle atrophy (Figure 4C). These results suggest that *Znf216* expression is associated with atrophy in skeletal muscles.

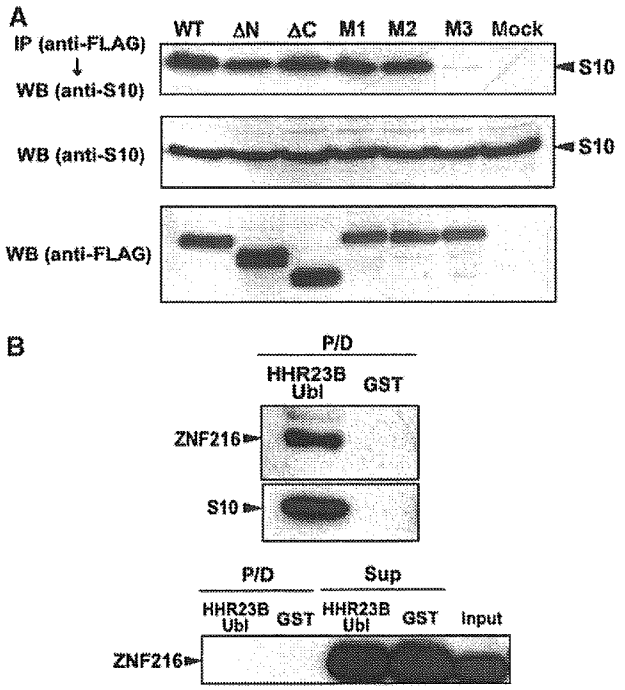

Figure 2 Interaction of ZNF216 with the 26S proteasome in mammalian cells. (A) Co-precipitation of the 26S proteasome and ZNF216. Co-precipitated proteins with FLAG-ZNF216 were resolved by SDS–PAGE and detected by immunoblotting using anti-S10a/Rpn7p antibody (anti-S10) or anti-FLAG antibody. Aliquots of cellular extracts were immunoblotted without immunoprecipitation to evaluate protein expression in the bottom panels. (**B**) ZNF216 was detected in the 26S proteasome fraction. Upper panel, cell lysates were incubated with a GST fusion of HHR23B Ubl (HHR23B Ubl) to isolate the 26S proteasome. Precipitated proteins (P/D) were separated and probed with anti-S10 or anti-ZNF216 antibody. Lower panel: purified recombinant ZNF216 was incubated with a GST fusion of HHR23B Ubl or GST protein. Precipitated (P/D) or not precipitated (Sup) proteins were probed with anti-ZNF216 antibody. No direct binding of ZNF216 to the Ubl domain of HHR23B was detected.

The transcription factor FOXO has been reported to play a critical role in muscular atrophy by inducing atrophy-related genes, including MAFbx/Atrogin-1 (Sandri *et al*, 2004; Stitt *et al*, 2004). Therefore, we asked whether FOXO activation upregulated *Znf216* expression. To do so, we employed a Cre-loxP system (Furukawa-Hibi *et al*, 2002) in which constitutively active FOXO4 (AFX-TM) created by mutation of the three Akt phosphorylation sites, T32A, S253A and S315A (Brunet *et al*, 1999), was expressed in C2C12-AFX-TM cells following infection by Cre recombinase-expressing adenovirus (Cre) (Figure 4D). Both AFX-TM mRNA and protein were induced 24 h after infection with Cre but not with control adenovirus (Furukawa-Hibi *et al*, 2002). ZNF216 mRNA was markedly increased in C2C12-AFX-TM cells as a result of infection with Cre but not following infection with control virus (Figure 4E). These results suggest that ZNF216 may function as a downstream effector of FOXO in muscle atrophy.

Generation of mice lacking ZNF216

To investigate the *in vivo* function of ZNF216, mice deficient for ZNF216 ($Znf216^{lex/lex}$) were generated by gene trapping at Omnibank of Lexicon Genetics (Zambrowicz *et al*, 1998). The structure of the predicted trapped gene is shown in Figure 5A. The trapping vector, VICTR48, was inserted 3.3 kbp upstream of exon 3, which encodes the first methionine of mouse *Znf216* (Figure 5A). $Znf216^{lex/lex}$ mice were born from interbred heterozygous $Znf216^{+/lex}$ mice in Mendelian ratios, indicating that ZNF216 is dispensable for embryogenesis or fetal development. No ZNF216 mRNA or protein was detected in $Znf216^{lex/lex}$ mice by Northern or immunoblot analyses, respectively (Figures 5B and C), indicating that the mice are ZNF216 nulls. Expression levels of ZNF216 in $Znf216^{+/lex}$ heterozygotes were nearly one-half those of wild-type mice. $Znf216^{lex/lex}$ mice were viable and fertile, without gross abnormalities or apparent pathological alteration, but they weighed less than sex- and age-matched controls (Figure 5D). At 45 weeks, the average weights of $Znf216^{+/+}$ and

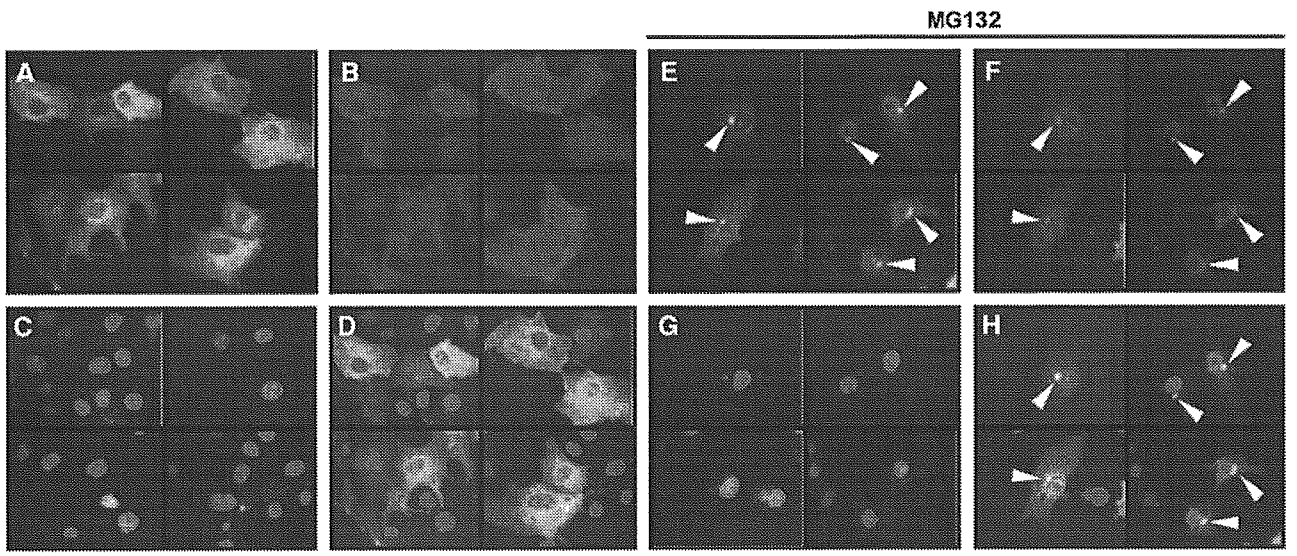

Figure 3 ZNF216 is localized in 'aggresomes' with ubiquitinylated proteins. (**A–H**) COS cells were transfected with expression vectors for FLAG-tagged ZNF216 and HA-tagged ubiquitin. Fixed cells were subjected to indirect immunofluorescence using (A, E) anti-FLAG (with AlexaFluor 488 anti-mouse IgG, green) and (B, F) anti-HA (with AlexaFluor 546 anti-rat IgG antibodies, red) antibodies. (C, G) Nuclei were stained with DAPI in the same fields of each panel. (E–H) Transfected COS cells were treated with the proteasome inhibitor, MG132 (0.5 μM). Aggresomes formed are indicated by arrowheads. The merged images were shown in (D and H).

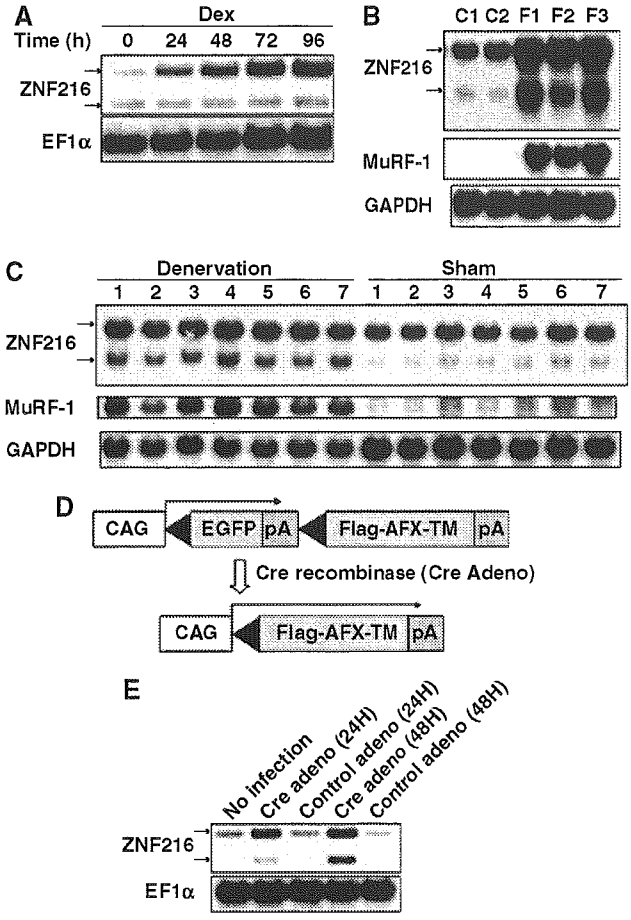

Figure 4 Expression of ZNF216 is induced by muscle atrophy. (**A**) C2C12 myoblast cells were differentiated into myotubes, and treated with 100 μM Dex for the indicated times. Northern blotting was performed to reveal the effect of Dex on ZNF216 expression. The entire coding region of ZNF216 was used as a probe, which recognized 2.4 and 1.5 kb mRNA species arising from alternative splicing and polyadenylation. The loading control was elongation factor α (EF1α). (**B**) Fasting-induced muscle atrophy. Three mice were fasted (F1 ~ F3), and two mice (C1, C2) were fed freely. After 2 days, RNA was purified from gastrocnemius muscle, and Northern blotting was performed to determine ZNF216 expression. The membrane was re-probed with MuRF-1 and GAPDH. (**C**) Denervation-induced muscle atrophy was induced by cutting the sciatic nerve of the hindlimb of seven mice (1 ~ 7). The opposite limb was sham operated as the control. At 7 days after surgery, total RNA was purified from gastrocnemius muscles, and Northern blotting was performed to detect ZNF216 expression. The membrane was re-probed with MuRF-1 and GAPDH. (**D**) Cre-loxP-mediated, constitutively active FOXO expression system. cDNA encoding FLAG-tagged constitutively active FOXO4 (AFX-TM) is separated from the CAG promoter of an expression vector by a loxP-flanked EGFP-poly(A) cassette. Infection with adenovirus expressing Cre recombinase (Cre) results in excision of the DNA fragment located between the two loxP sequences and expression of FLAG-tagged AFX-TM. (**E**) ZNF216 is downstream of FOXO. Total RNAs were prepared from C2C12-AFX-TM cells at the indicated times after infection with adenovirus expressing Cre (Cre) or lacZ (control) and probed by *Znf216* or EF1α. A marked increase in expression of *Znf216* was observed only in Cre-infected cells.

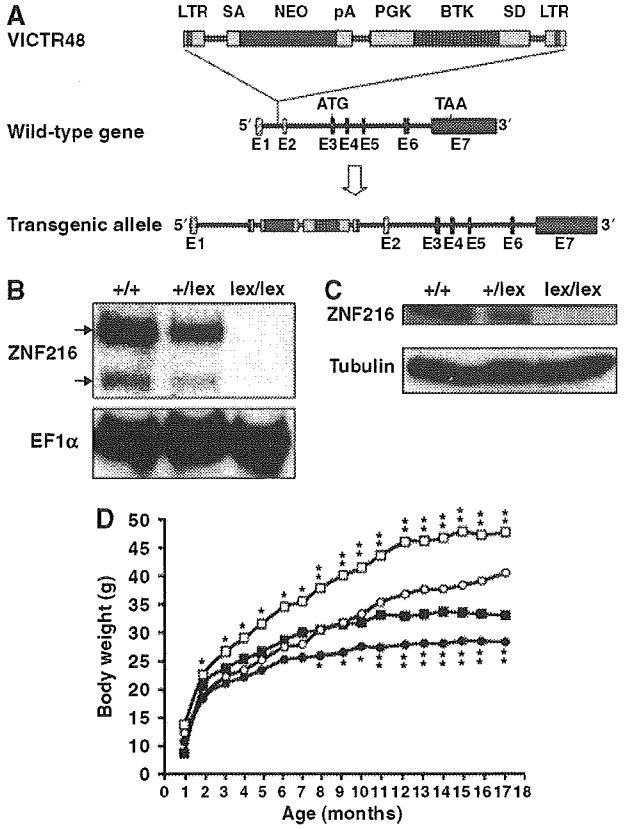

Figure 5 Disruption of *Znf216* gene in mice. (**A**) Gene trap strategy of *Znf216* gene. The structure of the trapping vector, VICTR48, is shown in the upper line. The wild-type allele and the trapped, transgenic allele follow the vector. The retroviral vector, VICTR48, was integrated between exons 1 and 2 of the *Znf216* gene and transcription of downstream exons encoding ZNF216 was diminished. Exons are depicted by striped (noncoding exons) or shadowed boxes (protein-coding exons) and numbered (E1 and E2). LTR, long terminal repeat; SA, splice acceptor site; SD, splice donor site; pA, polyadenylation signal; PGK, PGK promoter. (**B**) Northern blot analysis. Total RNA was prepared from brains of $Znf216^{+/+}$, $ZnfF216^{+/lex}$ or $Znf216^{lex/lex}$ mice. Full-length mouse ZNF216 cDNA was used as a probe. The membrane was re-probed using an EF1α probe. (**C**) Immunoblot analysis. Extracts from brain of $Znf216^{+/+}$, $Znf216^{+/lex}$ or $Znf216^{lex/lex}$ mice were immunoblotted with antibody against ZNF216. The membrane was re-probed using anti-tubulin antibody. (**D**) Growth curve of $Znf216^{lex/lex}$ mice. Body weights at each time point of $Znf216^{+/+}$ and $Znf216^{lex/lex}$ mice were indicated as open square boxes (males) or circles (females) and closed square boxes (males) or circles (females), respectively. $^{*}P<0.05$; $^{**}P<0.005$.

$Znf216^{lex/lex}$ male mice were 42.66 ± 7.06 g ($n = 14$) and 33.16 ± 4.44 g ($n = 9$), respectively. The average weights of female $Znf216^{+/+}$ and $Znf216^{lex/lex}$ mice were 34.46 ± 4.21 g ($n = 14$) and 26.85 ± 5.38 g ($n = 11$), respectively. After 30 weeks, both female and male $Znf216^{lex/lex}$ mice showed no or subtle increases in weight, whereas $Znf216^{+/+}$ or $Znf216^{+/lex}$ mice gained weight as they aged (Figure 5D). The size of most organs in $Znf216^{lex/lex}$ mice was reduced in proportion with body weight. However, the fat volume of aged (>30 weeks of age) $Znf216^{lex/lex}$ mice was significantly decreased, suggesting that the marked difference in body weight between wild-type and aged $Znf216^{lex/lex}$ mice is mainly caused by decreased fat mass seen in $Znf216^{lex/lex}$ mice (not shown). Detailed phenotypic characterization of aged mutant mice will be provided elsewhere.

Znf216$^{lex/lex}$ mice exhibit partial resistance to denervation-induced muscle atrophy

To further explore the involvement of ZNF216 in muscle atrophy, neurectomy of sciatic nerve was undertaken in wild-type and $Znf216^{lex/lex}$ mice. As shown in Figure 6A, 7

days after denervation, significant muscle weight loss and reduction in fiber sizes of the gastrocnemius muscle were observed in wild-type mice. By contrast, such decreases in muscle weight were significantly attenuated in *Znf216*$^{lex/lex}$ mice (Figure 6A). Sections of gastrocnemius muscle also showed larger fibers in muscle from neurectomized *Znf216*$^{lex/lex}$ mice than in control muscle (Figure 6B). However, there was no significant difference in fiber area between sham-operated wild-type and *Znf216*$^{lex/lex}$ mice (wild type + sham operated, $1988 \pm 530\,\mu m^2$; wild type + denervation, $1379 \pm 345\,\mu m^2$; lex/lex + sham operated, $1776 \pm 484\,\mu m^2$; lex/lex + denervation, $1393 \pm 344\,\mu m^2$). As shown in Figure 6C, the reduction in fiber area was also less apparent in *Znf216*$^{lex/lex}$ mice compared to wild-type mice. These results suggest that ZNF216 plays a crucial role in reduction of muscle mass on denervation-induced muscle atrophy.

Abnormal accumulation of ubiquitinylated proteins in muscle from Znf216$^{lex/lex}$ mice

To investigate what abnormalities occur during denervation-induced muscle atrophy in *Znf216*$^{lex/lex}$ mice, we examined expression levels of factors involved in muscle atrophy. As expected, expression of MAFbx/Atrogin-1 and MuRF-1 was dramatically induced by denervation-induced muscle atrophy in gastrocnemius muscle from wild-type mice (Figure 6A). In *Znf216*$^{lex/lex}$ mice, expression of MAFbx/Atrogin-1 and MuRF-1 was also induced at levels comparable to those seen in wild-type mice. Induction of *Pmsa1* and *Pmsd11*, genes encoding the 26S proteasome subunits α6 and Rpn6, respectively, was also indistinguishable between *Znf216*$^{lex/lex}$ and wild-type mice (Figure 7A). Furthermore, proteasome activities in gastrocnemius muscles were comparable between wild-type and *Znf216*$^{lex/lex}$ mice (Figure 7B). Thus, induction of relevant ubiquitin ligases or proteasome components was not affected in *Znf216*$^{lex/lex}$ mice. It is known that ubiquitinylated proteins accumulate during muscle atrophy (Medina *et al*, 1991; Wing *et al*, 1995). As shown in Figure 7C, following denervation, ubiquitinylated proteins accumulated in the gastrocnemius muscle of wild-type mice, but higher levels of ubiquitinylated proteins accumulated in muscle derived from *Znf216*$^{lex/lex}$ mice (~2-fold: $P<0.001$ in neurectomized *Znf216*$^{lex/lex}$ versus wild-type muscle). Similar results were obtained by fasting-induced muscle atrophy, although no difference in the levels of ubiquitinylated proteins from controls (sham-operated or fed) was observed between genotypes (Figure 7C). These results indicate that ZNF216 is a critical regulator of muscle atrophy, most likely functioning to regulate degradation of muscle proteins without altering expression of proteasomal components or known E3 ligases.

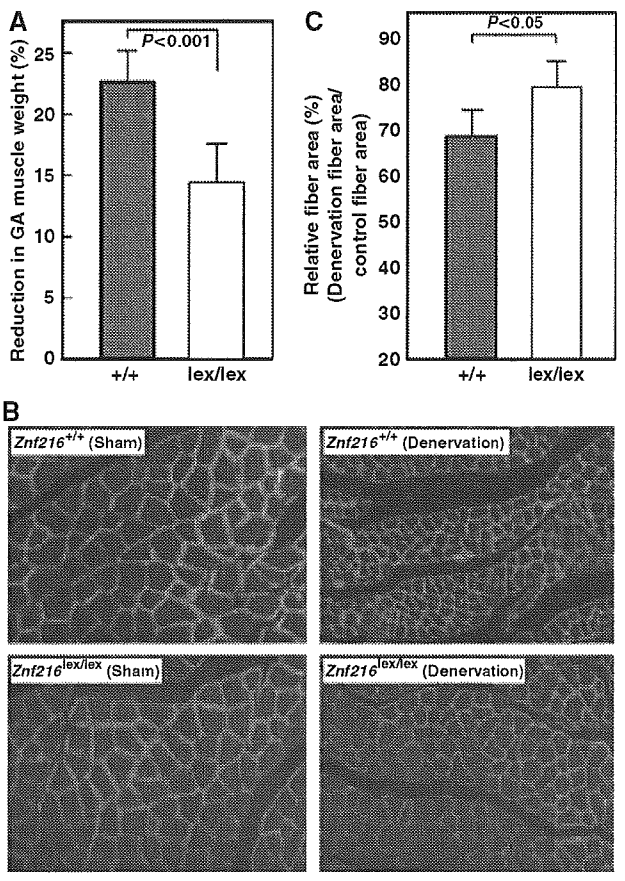

Figure 6 Denervation induced muscular atrophy was attenuated in *ZNF216*$^{lex/lex}$ mice. (**A**) Reduction of GA muscle weight upon neurectomy. Percent decreases in muscle weights are shown as a percent of control, calculated as the left/right muscle weights. (**B**) Cross-sections from gastrocnemius muscle were stained by indirect immunofluorescence with anti-laminin. The reduction in size was also significant in muscle fibers of control mice but less in *Znf216*$^{lex/lex}$. (**C**) Muscle fiber cross-sectional areas were measured in transverse tissue section (B). Percent relative fiber area of denervated muscle to control fiber area (sham-operated) are shown.

Effect of ZNF216 on UPS-mediated protein degradation

Accumulation of ubiquitinylated protein under any circumstance might be because of loss of inhibition of ubiquitinylation and/or deubiquitinylation (DUB). However, no inhibition or DUB activity was observed (Supplementary Figures S4 and S5). As shown in Figure 7D, association of ZNF216 protein to the proteasome was significantly increased when atrophy was induced, suggesting that ZNF216 may be involved in association of ubiquitinylated proteins and the proteasome. The biochemical activity of ZNF216 is similar to that of the UPS proteins, hHR23 and hPLIC, both of which have a shuttle function and are known to bind to both polyubiquitinylated proteins and the 26S proteasome (Hartmann-Petersen and Gordon, 2004; Elsasser and Finley, 2005). Interestingly, overexpression of hHR23 and hPLIC results in stabilization of unstable proteins such as p53 (Kleijnen *et al*, 2000; Glockzin *et al*, 2003). To determine if ZNF216 functioned similarly, we employed a degradation system using unstable GFP (Bence *et al*, 2001). In this system, the CL1 peptide, which functions as a degron, is fused to EGFP (EGFP-CL1). Degradation by conjugation with the degron is mediated by the UPS (Bence *et al*, 2001). EGFP-CL1, constitutively expressed in HEK293 cells, is unstable and the estimated half-life ($t_{1/2}$) of EGFP-CL1 in this system is about 11 min. Ubiquitinylated EGFP-CL1 protein stabilized by treatment with a proteasome inhibitor was associated with ZNF216 but EGFP itself was not (not shown). As shown in Figure 8A, protein degradation was markedly retarded in the presence of ectopic ZNF216 ($t_{1/2}>30$ min) compared to cells transfected with the loss of function mutant ZNF216M3 or mock-transfected cells. Rapid turnover of EGFP-CL1 protein was inhibited by treatment with the

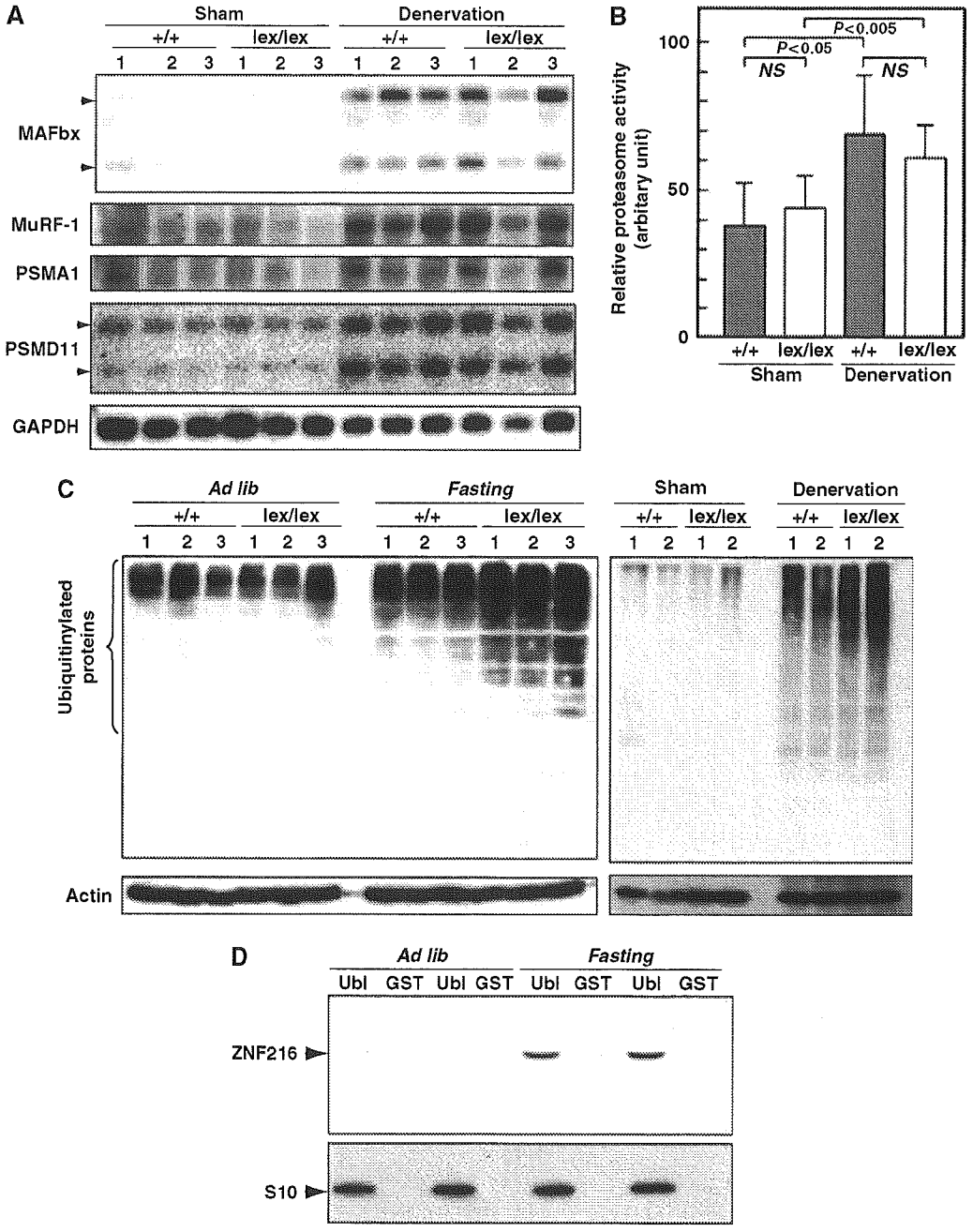

Figure 7 Changes in UPS upon muscular atrophy. (**A**) Expression of UPS components in denervation-induced muscular atrophy. Total RNAs were purified from gastrocnemius muscle, and Northern blotting was performed using indicated probes. Expression of genes for ubiquitin-ligases, such as MAFbx or MuRF-1, and proteasome subunits PSMA1 and PSMD11 was induced by muscle atrophy at comparable levels between wild-type and *ZNF216*$^{lex/lex}$ mice. (**B**) Proteasome activity. Proteasome activities in muscle extracts from wild-type or *ZNF216*$^{lex/lex}$ mice were measured and are shown as arbitrary units. No significant difference in proteasome activity between wild-type and *ZNF216*$^{lex/lex}$ was observed. (**C**) High levels of ubiquitinylated proteins accumulated in muscles from *ZNF216*$^{lex/lex}$ mice than in muscles from wild-type mice. Muscle extracts from wild-type or *ZNF216*$^{lex/lex}$ mice were subjected to immunoblotting using anti-ubiquitin antibody to analyze levels of ubiquitinylated proteins. Left and right panels show fasting-induced and denervation-induced muscle atrophy, respectively. Each membrane was re-probed with anti-actin antibody. (**D**) Association of ZNF216 with the proteasome was increased upon atrophy. The proteasome fractions in muscle extracts from fed (*ad lib*) or fasted (fasting) mice were precipitated with GST-Ubl or GST only as a negative control. Endogenous ZNF216 protein was co-precipitated with the proteasome, which is probed by the anti-S10 antibody.

proteasome inhibitor MG132 (MG132, Figure 8B). The levels of the proteins stabilized by MG132 were comparable among cells transfected with ZNF216 constructs, indicating that protein synthesis of EGFP-CL1 was not significantly affected by ectopic expression of ZNF216 (MG132, Figure 8B). ZNF216WT, and to a lesser extent the mutants M1 and M2 but not M3, attenuated degradation (NT, Figure 8B). Thus, as is the case with other shuttle proteins, overexpression of ZNF216 inhibits degradation of unstable proteins via the UPS.

Discussion

ZNF216 is an atrogene

In this report, we show that *Znf216*$^{lex/lex}$ mice exhibit resistance to denervation-induced muscle atrophy. It has been

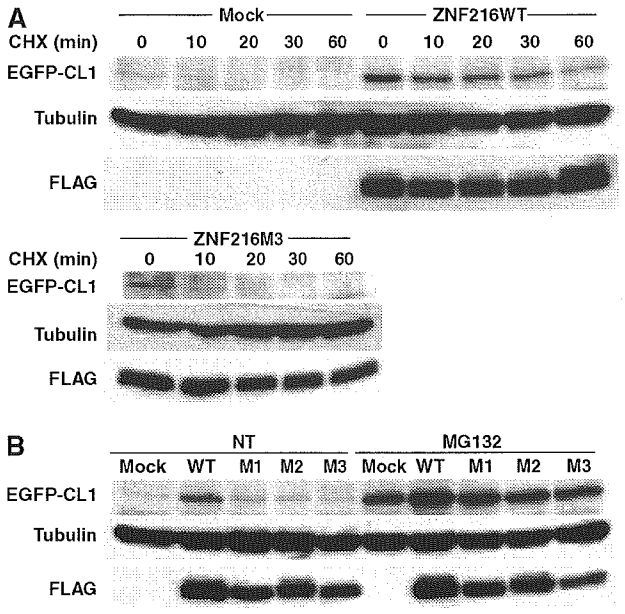

Figure 8 Ectopic expression of ZNF216-affected protein degradation. (A) Degradation of EGFP-CL1 protein was delayed by overexpression of ZNF216. 293 cells stably expressing EGFP-CL1 were transfected with plasmid of ZNF216WT, ZNF216M3 or pcDNA3 (mock). Estimated half-lives of the EGFP-CL1 are 35, 11 and 11 min in ZNF216WT-, ZNF216M3- and mock-transfected cells, respectively. *De novo* protein synthesis was arrested by cycloheximide (CHX). The membrane was re-probed with tubulin antibody to control for protein loading (tubulin) and FLAG antibody to detect ZNF216 expression (FLAG). (B) Degradation of EGFP-CL1 protein in the presence of various ZNF216 constructs. HEK293 cells stably expressing EGFP-CL1 were transfected with plasmids expressing the indicated mutants. Transfected cells were not treated (NT) or MG132-treated (MG132), and EGFP-CL1 protein was detected with an anti-GFP antibody (EGFP-CL1). The membrane was re-probed with tubulin antibody to control for protein loading (tubulin) and FLAG antibody to detect ZNF216 expression (FLAG).

shown that TNFα induces catabolic conditions through UPS during cancer cachexia (Mitch and Price, 2001). Recently, it has been reported that mice deficient in molecules involved in the NF-κB pathway exhibit resistance to muscular atrophy (Cai *et al*, 2004; Hunter and Kandarian, 2004; McKinnell and Rudnicki, 2004). On the other hand, the IGF-FOXO axis has been suggested to regulate muscle mass through induction of 'atrogenes' such as Murf1 and MAFbx/Atrogin-1 (Sandri *et al*, 2004; Stitt *et al*, 2004). Although we provide evidence that *Znf216* is downstream of FOXO, the NF-κB pathway could represent an alternative signal inducing ZNF216. Indeed, we have identified *Znf216* as a gene induced by RANKL, a TNF family ligand (Hishiya *et al*, 2005) which activates the NF-κB pathway through RANK (Anderson *et al*, 1997; Lacey *et al*, 1998). Moreover, TNFα and IL-1β upregulate expression of ZNF216 in fibroblasts and macrophages (Hishiya *et al*, 2005). These results suggest that *Znf216* may be activated by NF-κB. Huang *et al* (2004) recently reported that ZNF216 inhibits the NF-κB pathway. Whereas treatment with TNFα or overexpression of TRAF6 dramatically activated a reporter driven by NF-κB response elements, ectopic expression of A20/TNFAIP3 but not ZNF216 inhibited NF-κB activation (not shown). Using mouse embryonic fibroblasts, splenocytes or bone marrow cells from $Znf216^{lex/lex}$ or wild-type mice, no significant differences were observed in TNFα-dependent NF-κB activation, LPS-induced cytokine expression or proliferation (unpublished data). Therefore, ZNF216 seems to function as a downstream effector (i.e., a component of the UPS) rather than a specific negative regulator of NF-κB signaling, although ZNF216 function in that pathway is still under investigation. Whereas expression of ZNF216 is not restricted to muscle, such expression was induced upon muscular atrophy and loss of function of *Znf216* promotes resistance to denervation-induced atrophy, thereby suggesting that it fulfills the definition of an 'atrogene'.

As it is in skeletal muscle, ZNF216 is highly expressed in the brain (Scott *et al*, 1998). Aberrations in the UPS have been documented in the pathogenesis of neurodegenerative diseases such as Parkinson's and Huntington's diseases (Ross and Poirier, 2004). Massive accumulation of ubiquitinylated proteins, which are often aggregated and impair the UPS leading to neuronal degeneration, has been observed in these pathogenic conditions (Ciechanover and Brundin, 2003; Korhonen and Lindholm, 2004). In cultured cells, blocking the UPS by proteasome inhibitors leads to accumulation of ubiquitinylated proteins. These ubiquitinylated proteins are then transferred to perinuclear locations and form aggresomes (Johnston *et al*, 1998). As shown here, ZNF216 is localized in aggresomes together with ubiquitinylated proteins. Interestingly, proteomic analysis of a protein complex containing HDAC6, a protein often associated with aggresomes (Kawaguchi *et al*, 2003), showed that the complex included AWP1, a structural homologue of ZNF216 (Seigneurin-Berny *et al*, 2001). Although it is unclear whether ZNF216 is involved in aggresome formation, there is great interest in the role of ZNF216 in the pathogenesis of neurodegenerative diseases.

Molecular function of an A20-containing protein, ZNF216

In muscle atrophy, more ubiquitinylated proteins accumulate in muscle from $Znf216^{lex/lex}$ mice than in muscle from wild-type mice, suggesting an abnormal UPS function. Inhibition of neither polyubiquitinylation nor DUB activity was observed in ZNF216. Although our *in vivo* data showed significant accumulation of polyubiquitinylated proteins in muscle from $Znf216^{lex/lex}$ mice, there is a possibility that ZNF216 is a ubiquitin-ligase. It has been recently reported that A20/TNFAIP3 protein possesses ubiquitin ligase activity against RIP through its ZnF-A20 repeats (Wertz *et al*, 2004). We asked whether the ZnF-A20 of ZNF216 exhibited activity similar to A20/TNFAIP3, but *in vitro* ubiquitinylation assays were negative (Supplementary Figure S6). In fact, the ZnF-A20 of A20/TNFAIP3 protein does not bind polyubiquitin chains as does the ZnF-A20 of ZNF216 (Supplementary Figure S1). Furthermore, there are seven ZnF-A20 motifs in A20/TNFAIP3 and only the fourth is responsible for E3 activity, suggesting that the ZnF-A20 motif is not inherently active enzymatically (Wertz *et al*, 2004). However, we cannot exclude the possibility that ZNF216 may possess DUB or E3 activity highly specific to an unknown substrate without nonspecific or self-ubiquitinylating activity.

ZNF216 likely acts as a bridging or a shuttle factor of ubiquitinylated proteins targeted to the proteasome. Shuttle proteins, such as Rad23p and Dsk2p, share interfaces for ubiquitinylated proteins and the proteasome (Hartmann-Petersen and Gordon, 2004; Elsasser and Finley, 2005).

Although shuttle proteins are required for efficient protein degradation, ectopic expression of hHR23 or hPLIC, the human homologues of Rad23p or Dsk2p, respectively, lead to stabilization of p53 protein (Kleijnen *et al*, 2000; Glockzin *et al*, 2003). These outcomes may be caused by titration effects due to overexpression and are commonly observed following misexpression of shuttle proteins in yeast and mammals (Hartmann-Petersen and Gordon, 2004; Verma *et al*, 2004). Here, we show that ZNF216 has a ubiquitin binding domain and can associate with the 26S proteasome even in the absence of ubiquitin binding, and that overexpression of the zinc-finger protein attenuates protein degradation rate. There is no structural counterpart of ZNF216 in the yeast genome. We asked whether ZNF216 could rescue the bridging function of RAD23 or DSK2 mutants by introducing ZNF216 into Δ*rad23*Δ*dsk2* yeast cells, but the phenotype could not be rescued (data not shown). This suggests that ZNF216 is not the functional orthologue of these proteins. Recently, the presence of an alternative pathway of Rad23p/Dsk2p in protein targeting to the proteasome has been suggested (Bazirgan and Hampton, 2005; Richly *et al*, 2005). It has been reported that tetra-ubiquitin constitutes the minimum proteasomal targeting signal and that the length of polyubiquitin chain may determine the targeting route (Thrower *et al*, 2000; Bazirgan and Hampton, 2005; Richly *et al*, 2005). Notably, ZNF216 preferentially binds polyubiquitin chains longer than di- or tri-ubiquitin (Figure 1D). Therefore, these data suggest that ZNF216 is a novel ubiquitin recognition factor, required for efficient protein degradation via a pathway different from the canonical Rad23p/Dsk2p pathway. Although it is now under investigation, the characterization of ZnF-AN1, an AN1-type zinc-finger domain located at the C-terminus of ZNF216, may reveal the precise molecular function of ZNF216.

Materials and methods

Antibodies

An anti-ZNF216 antibody was raised by immunizing rabbits against synthesized peptide corresponding to the C-terminal sequence of mouse ZNF216. Mouse monoclonal antibodies for FLAG (Sigma, St Louis, MO) and ubiquitin (Santa Cruz Biotechnology, CA), rabbit polyclonal antibodies for ubiquitin (Affiniti Research Products) and actin (Neo Markers, CA), a rat monoclonal antibody for HA (Roche Diagnostics, Mannheim, Germany), and a rabbit polyclonal antibody against S10a/Rpn7p (Affiniti Research Products) were purchased from the indicated manufacturers. For indirect immunofluorescence staining, AlexaFluor 488 goat anti-mouse IgG or AlexaFluor 546 goat anti-rat IgG antibody was obtained from Molecular Probes, OR.

Identification of interacting proteins

RNA was purified from RAW264.7 cells stimulated by RANKL, and used to construct the yeast library (MatchMaker Library Construction & Screening Kit, Clontech). Yeast two-hybrid screening with pGBKT7-ZNF216 was performed as described previously (Masuda *et al*, 2001). Identification of the co-immunoprecipitated proteins with N- or C-terminally FLAG-tagged ZNF216 (ZA20D2) or AWP1 (ZA20D3) was essentially done by a nano-LC/MS/MS system as previously described (Natsume *et al*, 2002; Komatsu *et al*, 2004).

Experimental models of muscle atrophy

For fasting-induced muscle atrophy, 8-week-old C57BL6 male mice were deprived of food but given free access to water. After 2 days, gastrocnemius muscles were harvested for each experiment. Denervation-induced muscle atrophy was performed by dissecting the sciatic nerve of one hindlimb, and the other hindlimb was sham operated as the control. After 7 days, the contralateral normal and denervated gastrocnemius muscles were harvested for each experiment. All animal experiments were approved in advance by the Ethics Review Committee for Animal Experimentation of the National Institute for Longevity Sciences and the National Center for Geriatrics and Gerontology. Student's *t*-tests were used to evaluate statistical differences between the two groups.

Znf216-deficient mice

Generation of heterozygous *Znf216*$^{+/lex}$ mice was essentially done by the gene trap method at Lexicon Genetics (Zambrowicz *et al*, 1998). Briefly, ES cells heterozygous for the trapped *Znf216* gene were microinjected into eight-cell-stage ICR mouse embryos and transplanted into uteri. Chimeric mice were crossed to C57BL/6J mice. Northern and immunoblot analyses confirmed disruption of the gene (see text). For genotyping, primers were as follows: KO-A, ACCGACAGGATAGACAATGGCAGAG; KO-B, CGATTTTAAGAAAG GAGGCTCTGACC; LTR2, AAATGGCGTTACTTAAGCTAGCTTGC. The wild-type and inserted alleles were detected by PCR using KO-A and KO-B (0.5 kb), and LTR2 and KO-B (0.3 kb), respectively.

EGFP-CL1 degradation assay

The nucleotide sequence encoding the CL1 peptide (ACKNWFSSLSHFVIHL) (Gilon *et al*, 1998) was inserted into the *Xho*I/*Eco*RI site of pEGFP-C3, and the resulting plasmid was designated pEGFP-CL1. A cell line stably expressing EGFP-CL1 (293EGFP-CL1) was generated by transfection of pEGFP-CL1 into 293 cells. For the degradation assay, ZNF216 expression vectors were transfected into 293EGFP-CL1 cells and cells were harvested 48 h after transfection. MG132 (final 10 μM) or cycloheximide (final 100 μg/ml) was added to the culture at 12 or 1 h before harvest, respectively. Protein extraction was as described above.

For more details on supplementary Materials and methods, see Supplementary data

Supplementary data

Supplementary data are available at *The EMBO Journal* Online.

Acknowledgements

We are grateful to Drs Kazuhiro Iwai (Osaka City University) and Noboru Motoyama (NCGG) for reagents, helpful comments and suggestions throughout this study. We also thank Drs Akio Matsuda and Tatsuo Furuyama for experimental instruction and advice; Dr Aya Sasaki for pathological determinations; Ms Miho Kamiya and Ms Kumi Tsutsumi for technical assistance; and Dr Elise Lamar for proofreading the manuscript. This study is supported in part by the Program for Promotion of Fundamental Studies in Health Sciences of the Organization for Pharmaceutical Safety and Research of Japan, and by a Research Grant for Longevity Sciences from the Ministry of Health, Labor and Welfare.

References

Anderson DM, Maraskovsky E, Billingsley WL, Dougall WC, Tometsko ME, Roux ER, Teepe MC, DuBose RF, Cosman D, Galibert L (1997) A homologue of the TNF receptor and its ligand enhance T-cell growth and dendritic-cell function. *Nature* **390:** 175–179

Bailey JL, Wang X, England BK, Price SR, Ding X, Mitch WE (1996) The acidosis of chronic renal failure activates muscle proteolysis in rats by augmenting transcription of genes encoding proteins of the ATP-dependent ubiquitin-proteasome pathway. *J Clin Invest* **97:** 1447–1453

Bazirgan OA, Hampton RY (2005) Cdc48-Ufd2-Rad23: the road less ubiquitinated? *Nat Cell Biol* **7:** 207–209

Bence NF, Sampat RM, Kopito RR (2001) Impairment of the ubiquitin-proteasome system by protein aggregation. *Science* **292:** 1552–1555

Bodine SC, Latres E, Baumhueter S, Lai VK, Nunez L, Clarke BA, Poueymirou WT, Panaro FJ, Na E, Dharmarajan K, Pan ZQ, Valenzuela DM, DeChiara TM, Stitt TN, Yancopoulos GD, Glass DJ (2001) Identification of ubiquitin ligases required for skeletal muscle atrophy. *Science* **294:** 1704–1708

Brunet A, Bonni A, Zigmond MJ, Lin MZ, Juo P, Hu LS, Anderson MJ, Arden KC, Blenis J, Greenberg ME (1999) Akt promotes cell survival by phosphorylating and inhibiting a Forkhead transcription factor. *Cell* **96:** 857–868

Cai D, Frantz JD, Tawa Jr NE, Melendez PA, Oh BC, Lidov HG, Hasselgren PO, Frontera WR, Lee J, Glass DJ, Shoelson SE (2004) IKKbeta/NF-kappaB activation causes severe muscle wasting in mice. *Cell* **119:** 285–298

Chen L, Shinde U, Ortolan TG, Madura K (2001) Ubiquitin-associated (UBA) domains in Rad23 bind ubiquitin and promote inhibition of multi-ubiquitin chain assembly. *EMBO Rep* **2:** 933–938

Ciechanover A, Brundin P (2003) The ubiquitin proteasome system in neurodegenerative diseases: sometimes the chicken, sometimes the egg. *Neuron* **40:** 427–446

Elsasser S, Finley D (2005) Delivery of ubiquitinated substrates to protein-unfolding machines. *Nat Cell Biol* **7:** 742–749

Funakoshi M, Sasaki T, Nishimoto T, Kobayashi H (2002) Budding yeast Dsk2p is a polyubiquitin-binding protein that can interact with the proteasome. *Proc Natl Acad Sci USA* **99:** 745–750

Furukawa-Hibi Y, Yoshida-Araki K, Ohta T, Ikeda K, Motoyama N (2002) FOXO forkhead transcription factors induce G(2)-M checkpoint in response to oxidative stress. *J Biol Chem* **277:** 26729–26732

Gilon T, Chomsky O, Kulka RG (1998) Degradation signals for ubiquitin system proteolysis in Saccharomyces cerevisiae. *EMBO J* **17:** 2759–2766

Glickman MH, Ciechanover A (2002) The ubiquitin-proteasome proteolytic pathway: destruction for the sake of construction. *Physiol Rev* **82:** 373–428

Glockzin S, Ogi FX, Hengstermann A, Scheffner M, Blattner C (2003) Involvement of the DNA repair protein hHR23 in p53 degradation. *Mol Cell Biol* **23:** 8960–8969

Gomes MD, Lecker SH, Jagoe RT, Navon A, Goldberg AL (2001) Atrogin-1, a muscle-specific F-box protein highly expressed during muscle atrophy. *Proc Natl Acad Sci USA* **98:** 14440–14445

Hartmann-Petersen R, Gordon C (2004) Protein degradation: recognition of ubiquitinylated substrates. *Curr Biol* **14:** R754–R756

Hershko A, Ciechanover A (1998) The ubiquitin system. *Annu Rev Biochem* **67:** 425–479

Hishiya A, Ikeda K, Watanabe K (2005) A RANKL-inducible gene Znf216 in osteoclast differentiation. *J. Receptor Signal Transduct* **25:** 199–216

Horiuchi H, Lippe R, McBride HM, Rubino M, Woodman P, Stenmark H, Rybin V, Wilm M, Ashman K, Mann M, Zerial M (1997) A novel Rab5 GDP/GTP exchange factor complexed to Rabaptin-5 links nucleotide exchange to effector recruitment and function. *Cell* **90:** 1149–1159

Huang J, Teng L, Li L, Liu T, Li L, Chen D, Xu LG, Zhai Z, Shu HB (2004) ZNF216 is an A20-like and IkappaB kinase gamma-interacting inhibitor of NFkappaB activation. *J Biol Chem* **279:** 16847–16853

Hunter RB, Kandarian SC (2004) Disruption of either the Nfkb1 or the Bcl3 gene inhibits skeletal muscle atrophy. *J Clin Invest* **114:** 1504–1511

Jagoe RT, Lecker SH, Gomes M, Goldberg AL (2002) Patterns of gene expression in atrophying skeletal muscles: response to food deprivation. *FASEB J* **16:** 1697–1712

Johnston JA, Ward CL, Kopito RR (1998) Aggresomes: a cellular response to misfolded proteins. *J Cell Biol* **143:** 1883–1898

Kawaguchi Y, Kovacs JJ, McLaurin A, Vance JM, Ito A, Yao TP (2003) The deacetylase HDAC6 regulates aggresome formation and cell viability in response to misfolded protein stress. *Cell* **115:** 727–738

Kleijnen MF, Shih AH, Zhou P, Kumar S, Soccio RE, Kedersha NL, Gill G, Howley PM (2000) The hPLIC proteins may provide a link between the ubiquitination machinery and the proteasome. *Mol Cell* **6:** 409–419

Komatsu M, Chiba T, Tatsumi K, Iemura S, Tanida I, Okazaki N, Ueno T, Kominami E, Natsume T, Tanaka K (2004) A novel protein-conjugating system for Ufm1, a ubiquitin-fold modifier. *EMBO J* **23:** 1977–1986

Kopito RR (2000) Aggresomes, inclusion bodies and protein aggregation. *Trends Cell Biol* **10:** 524–530

Korhonen L, Lindholm D (2004) The ubiquitin proteasome system in synaptic and axonal degeneration: a new twist to an old cycle. *J Cell Biol* **165:** 27–30

Lacey DL, Timms E, Tan HL, Kelley MJ, Dunstan CR, Burgess T, Elliott R, Colombero A, Elliott G, Scully S, Hsu H, Sullivan J, Hawkins N, Davy E, Capparelli C, Eli A, Qian YX, Kaufman S, Sarosi I, Shalhoub V, Senaldi G, Guo J, Delaney J, Boyle WJ (1998) Osteoprotegerin ligand is a cytokine that regulates osteoclast differentiation and activation. *Cell* **93:** 165–176

Lambertson D, Chen L, Madura K (1999) Pleiotropic defects caused by loss of the proteasome-interacting factors Rad23 and Rpn10 of *Saccharomyces cerevisiae*. *Genetics* **153:** 69–79

Lecker SH, Jagoe RT, Gilbert A, Gomes M, Baracos V, Bailey J, Price SR, Mitch WE, Goldberg AL (2004) Multiple types of skeletal muscle atrophy involve a common program of changes in gene expression. *FASEB J* **18:** 39–51

Lecker SH, Solomon V, Mitch WE, Goldberg AL (1999) Muscle protein breakdown and the critical role of the ubiquitin–proteasome pathway in normal and disease states. *J Nutr* **129:** 227S–237S

Lelouard H, Gatti E, Cappello F, Gresser O, Camosseto V, Pierre P (2002) Transient aggregation of ubiquitinated proteins during dendritic cell maturation. *Nature* **417:** 177–182

Masuda Y, Sasaki A, Shibuya H, Ueno N, Ikeda K, Watanabe K (2001) Dlxin-1, a novel protein that binds Dlx5 and regulates its transcriptional function. *J Biol Chem* **276:** 5331–5338

McKinnell IW, Rudnicki MA (2004) Molecular mechanisms of muscle atrophy. *Cell* **119:** 907–910

Medina R, Wing SS, Haas A, Goldberg AL (1991) Activation of the ubiquitin-ATP-dependent proteolytic system in skeletal muscle during fasting and denervation atrophy. *Biomed Biochim Acta* **50:** 347–356

Mitch WE, Goldberg AL (1996) Mechanisms of muscle wasting. The role of the ubiquitin-proteasome pathway. *N Engl J Med* **335:** 1897–1905

Mitch WE, Price SR (2001) Transcription factors and muscle cachexia: is there a therapeutic target? *Lancet* **357:** 734–735

Natsume T, Yamauchi Y, Nakayama H, Shinkawa T, Yanagida M, Takahashi N, Isobe T (2002) A direct nanoflow liquid chromatography-tandem mass spectrometry system for interaction proteomics. *Anal Chem* **74:** 4725–4733

Opipari Jr AW, Boguski MS, Dixit VM (1990) The A20 cDNA induced by tumor necrosis factor alpha encodes a novel type of zinc finger protein. *J Biol Chem* **265:** 14705–14708

Pickart CM, Cohen RE (2004) Proteasomes and their kin: proteases in the machine age. *Nat Rev Mol Cell Biol* **5:** 177–187

Price SR, Bailey JL, Wang X, Jurkovitz C, England BK, Ding X, Phillips LS, Mitch WE (1996) Muscle wasting in insulinopenic rats results from activation of the ATP-dependent, ubiquitin-proteasome proteolytic pathway by a mechanism including gene transcription. *J Clin Invest* **98:** 1703–1708

Richly H, Rape M, Braun S, Rumpf S, Hoege C, Jentsch S (2005) A series of ubiquitin binding factors connects CDC48/p97 to substrate multiubiquitylation and proteasomal targeting. *Cell* **120:** 73–84

Ross CA, Poirier MA (2004) Protein aggregation and neurodegenerative disease. *Nat Med* **10** (Suppl): S10–S17

Sacheck JM, Ohtsuka A, McLary SC, Goldberg AL (2004) IGF-I stimulates muscle growth by suppressing protein breakdown and expression of atrophy-related ubiquitin ligases, atrogin-1 and MuRF1. *Am J Physiol Endocrinol Metab* **287:** E591–E601

Saeki Y, Saitoh A, Toh-e A, Yokosawa H (2002) Ubiquitin-like proteins and Rpn10 play cooperative roles in ubiquitin-dependent proteolysis. *Biochem Biophys Res Commun* **293:** 986–992

Sandri M, Sandri C, Gilbert A, Skurk C, Calabria E, Picard A, Walsh K, Schiaffino S, Lecker SH, Goldberg AL (2004) Foxo transcription factors induce the atrophy-related ubiquitin ligase atrogin-1 and cause skeletal muscle atrophy. *Cell* **117:** 399–412

Scott DA, Greinwald Jr JH, Marietta JR, Drury S, Swiderski RE, Vinas A, DeAngelis MM, Carmi R, Ramesh A, Kraft ML, Elbedour K, Skworak AB, Friedman RA, Srikumari Srisailapathy CR, Verhoeven K, Van Gamp G, Lovett M, Deininger PL, Batzer MA, Morton CC, Keats BJ, Smith RJ, Sheffield VC (1998) Identification and mutation analysis of a cochlear-expressed, zinc finger

protein gene at the DFNB7/11 and dn hearing-loss loci on human chromosome 9q and mouse chromosome 19. *Gene* **215:** 461–469

Seigneurin-Berny D, Verdel A, Curtet S, Lemercier C, Garin J, Rousseaux S, Khochbin S (2001) Identification of components of the murine histone deacetylase 6 complex: link between acetylation and ubiquitination signaling pathways. *Mol Cell Biol* **21:** 8035–8044

Stitt TN, Drujan D, Clarke BA, Panaro F, Timofeyva Y, Kline WO, Gonzalez M, Yancopoulos GD, Glass DJ (2004) The IGF-1/PI3K/Akt pathway prevents expression of muscle atrophy-induced ubiquitin ligases by inhibiting FOXO transcription factors. *Mol Cell* **14:** 395–403

Tawa Jr NE, Odessey R, Goldberg AL (1997) Inhibitors of the proteasome reduce the accelerated proteolysis in atrophying rat skeletal muscles. *J Clin Invest* **100:** 197–203

Thrower JS, Hoffman L, Rechsteiner M, Pickart CM (2000) Recognition of the polyubiquitin proteolytic signal. *EMBO J* **19:** 94–102

Verma R, Oania R, Graumann J, Deshaies RJ (2004) Multiubiquitin chain receptors define a layer of substrate selectivity in the ubiquitin–proteasome system. *Cell* **118:** 99–110

Wertz IE, O'Rourke KM, Zhou H, Eby M, Aravind L, Seshagiri S, Wu P, Wiesmann C, Baker R, Boone DL, Ma A, Koonin EV, Dixit VM (2004) De-ubiquitination and ubiquitin ligase domains of A20 downregulate NF-kappaB signalling. *Nature* **430:** 694–699

Wilkinson CR, Ferrell K, Penney M, Wallace M, Dubiel W, Gordon C (2000) Analysis of a gene encoding Rpn10 of the fission yeast proteasome reveals that the polyubiquitin-binding site of this subunit is essential when Rpn12/Mts3 activity is compromised. *J Biol Chem* **275:** 15182–15192

Wing SS, Goldberg AL (1993) Glucocorticoids activate the ATP-ubiquitin-dependent proteolytic system in skeletal muscle during fasting. *Am J Physiol* **264:** E668–E676

Wing SS, Haas AL, Goldberg AL (1995) Increase in ubiquitin–protein conjugates concomitant with the increase in proteolysis in rat skeletal muscle during starvation and atrophy denervation. *Biochem J* **307** (Part 3): 639–645

Young P, Deveraux Q, Beal RE, Pickart CM, Rechsteiner M (1998) Characterization of two polyubiquitin binding sites in the 26 S protease subunit 5a. *J Biol Chem* **273:** 5461–5467

Zambrowicz BP, Friedrich GA, Buxton EC, Lilleberg SL, Person C, Sands AT (1998) Disruption and sequence identification of 2000 genes in mouse embryonic stem cells. *Nature* **392:** 608–611

JOURNAL OF VIROLOGY, July 2004, p. 7270–7273 Vol. 78, No. 13
0022-538X/04/$08.00+0 DOI: 10.1128/JVI.78.13.7270–7273.2004

Inhibition of Virus Production in JC Virus-Infected Cells by Postinfection RNA Interference

Yasuko Orba,[1,2] Hirofumi Sawa,[1,2,3]* Hiroshi Iwata,[1,2] Shinya Tanaka,[1,2] and Kazuo Nagashima[1,2]

Laboratory of Molecular and Cellular Pathology[1] and 21st Century COE Program for Zoonosis Control,[3] Hokkaido University Graduate School of Medicine, Kita-ku, Sapporo 060-8638, and CREST, JST, Sapporo,[2] Japan

Received 25 February 2004/Accepted 30 March 2004

RNA interference has been applied for the prevention of virus infections in mammalian cells but has not succeeded in eliminating infections from already infected cells. We now show that the transfection of JC virus-infected SVG-A human glial cells with small interfering RNAs that target late viral proteins, including agnoprotein and VP1, results in a marked inhibition both of viral protein expression and of virus production. RNA interference directed against JC virus genes may thus provide a basis for the development of new strategies to control infections with this polyomavirus.

JC virus (JCV) belongs to the polyomavirus family of double-stranded DNA viruses and causes progressive multifocal leukoencephalopathy (PML) in humans (23). PML is often observed in immunosuppressed individuals, such as those with AIDS or advanced malignancies. Although highly active antiretroviral therapy, which includes treatment with protease inhibitors, improves the survival rate of patients with AIDS-related PML (2, 7), current therapeutic approaches to PML are not satisfactory. Treatment with cytosine arabinoside (8) or cidofovir (15) has failed to prove efficacious in individuals with PML. Trials of topotecan, which inhibits DNA topoisomerase and blocks JCV replication in vitro (11), are currently under way in such individuals. RNA interference (RNAi) with small interfering RNAs (siRNAs) has recently become a widely used approach for repressing cellular or viral gene expression (5, 6, 10, 16). Although several studies have shown that virus infections can be prevented by a prior or concomitant administration of siRNAs, the elimination of established infections from cells or tissues by RNAi has not been demonstrated (1).

To attempt to inhibit JCV production in infected cells, we designed the following siRNAs (Dharmacon) to target three different JCV proteins (Fig. 1a): VP274 and VP691 for VP1, Ag122 and Ag147 for agnoprotein, and LT78 and LT134 for the large T antigen (T-Ag). The JCV early and late RNAs are generated by alternative splicing. The early RNAs encode T-Ag and the small t antigen (14), whereas the major late RNA encodes both agnoprotein and VP1 (21). We introduced the JCV-specific siRNAs into cells of the SVG-A (simian virus 40 [SV40]-transformed human fetal glial cells) line (13) that had been inoculated with JCV (Mad-1/SVEΔ strain; 1,024 hemagglutination activity units per 3×10^5 cells) 4 days previously. JCV late proteins, including VP1 and agnoprotein, were detected by an immunoblot analysis at 2 days postinfection (dpi) and were abundant at 4 dpi (Fig. 1b). At 4 and 6 dpi, each siRNA (120 pmol per 6×10^4 cells) was introduced individually into SVG-A cells by the use of Lipofectamine 2000 (Invitrogen) (Fig. 1c). About 80% of the SVG-A cells were successfully transfected with a fluorescein-conjugated Ag122 siRNA (data not shown). The abundance of JCV proteins in siRNA-transfected cells was examined 48 h after the second transfection by an immunoblot analysis with antibodies specific for agnoprotein (3, 18, 19), VP1 (12, 22), or SV40 T-Ag (Ab-2; Oncogene Research Products) (20). Cells transfected with Ag122, Ag147, or VP274 manifested a marked depletion of viral proteins compared with cells transfected with a control siRNA with a scrambled sequence which is not present in mammalian cells (Dharmacon) (Fig. 1d). Ag122 inhibited the expression of VP1 as well as that of agnoprotein in a dose-dependent manner, but it did not affect the abundance of T-Ag, lamin A/C, or actin (Fig. 1d and e). The antibodies to SV40 T-Ag did not allow for differentiation between JCV T-Ag and SV40 T-Ag in SV40-transformed cells, as these two proteins share >70% amino acid sequence identity (4). We therefore assessed the effects of LT78 and LT134 on JCV T-Ag expression by reverse transcription (RT) and PCR; the abundance of JCV T-Ag mRNA was not affected by the transfection of cells with either siRNA (data not shown).

We also examined the effects of Ag122 and VP274 siRNAs by an indirect immunofluorescence analysis in JCV-infected cells. At 48 h posttransfection, methanol-fixed cells were stained with antibodies to VP1 or agnoprotein and then with Alexa Fluor 488-conjugated goat antibodies to rabbit immunoglobulin G (Molecular Probes). Cells positive for VP1 or agnoprotein were visualized with a laser-scanning confocal microscope (Olympus) and counted in six fields of view. The proportion of agnoprotein-positive cells was significantly reduced for cells transfected with Ag122, VP274, or both siRNAs compared with the value for cells transfected with the scrambled siRNA (Fig. 2a). Similarly, the percentage of VP1-positive cells was also reduced by transfection with Ag122, VP274, or both Ag122 and VP274. We confirmed the inhibition of the expression of agnoprotein and VP1 in cells transfected with

* Corresponding author. Mailing address: Laboratory of Molecular and Cellular Pathology, Hokkaido University School of Medicine, N15, W7, Kita-ku, Sapporo 060-8638, Japan. Phone: 81-11-706-5053. Fax: 81-11-706-7806. E-mail: h-sawa@patho2.med.hokudai.ac.jp.

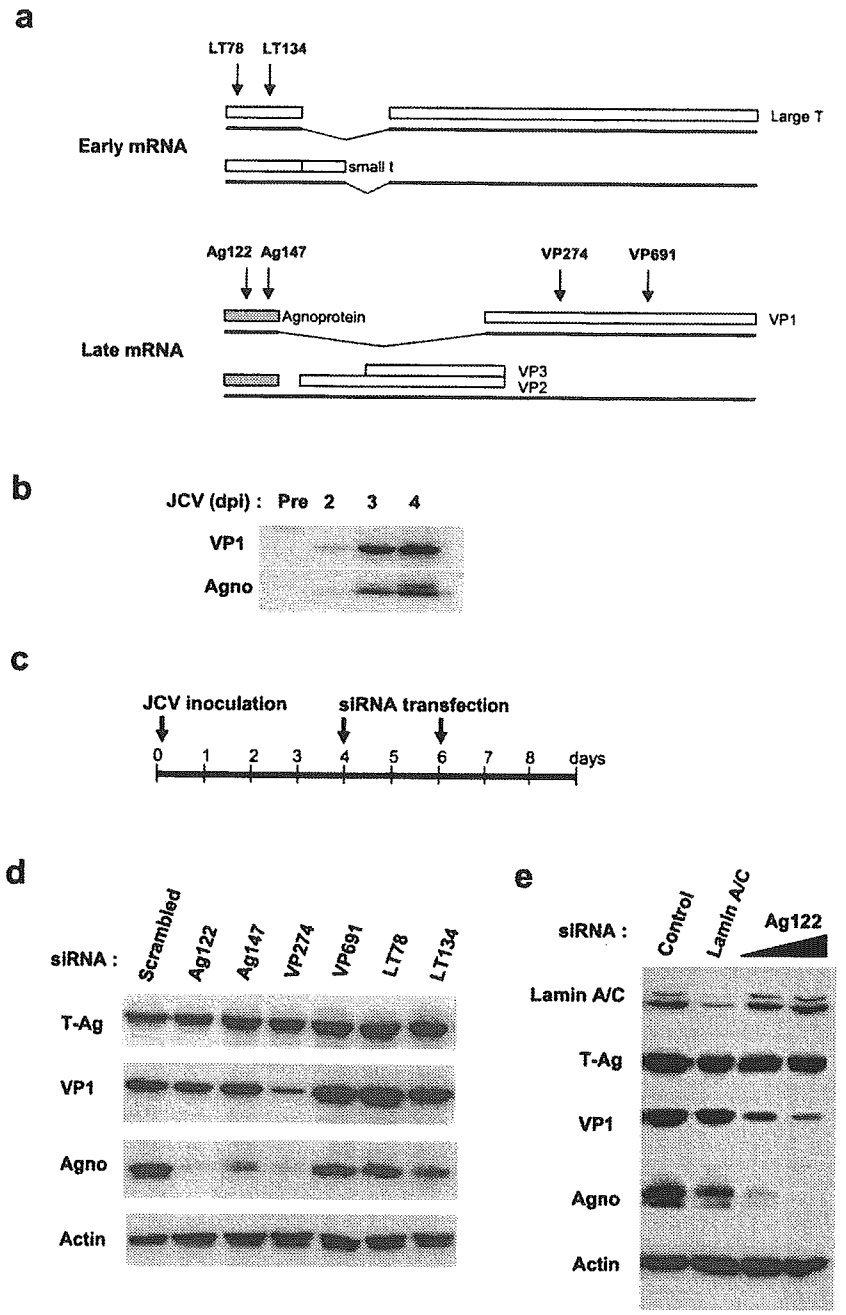

FIG. 1. Effects of postinfection RNAi on the abundance of JCV proteins in JCV-infected SVG-A cells. (a) Schematic representation of major early and late mRNAs of JCV. Major early mRNAs encode the small t antigen and T-Ag, which are translated as splicing variants. Two major forms of late mRNA encode either agnoprotein and VP1 or agnoprotein, VP2, and VP3. The regions of the viral RNAs targeted by the siRNAs are indicated by arrows. (b) Immunoblot analysis of the abundance of VP1 and agnoprotein of JCV in SVG-A cells at the indicated times after infection with JCV. (c) Schedule for JCV infection and siRNA transfection in SVG-A cells. (d) Immunoblot analysis of the indicated proteins in JCV-infected cells subjected to transfection with the indicated siRNAs. (e) Immunoblot analysis of the indicated proteins in JCV-infected cells subjected to transfection with the Ag122 siRNA at 60 or 120 pmol/well or with a lamin A/C-specific siRNA. Control (infected) cells were subjected to mock transfection.

Ag122, VP274, or both siRNAs by an immunoblot analysis (Fig. 2b). The extent of inhibition of viral protein expression achieved with the combination of Ag122 and VP274 did not differ significantly from that achieved with either siRNA alone. The observed inhibition of both agnoprotein and VP1 expression by either Ag122 or VP274 was likely due to the degradation of the polycistronic late RNA for both of these proteins induced by each siRNA.

It is thought that siRNAs target mRNAs containing the same sequences and induce their cleavage. We therefore examined the effects of Ag122 and VP274 on the abundance of JCV mRNAs. Total RNAs were isolated from cells 12 or 24 h

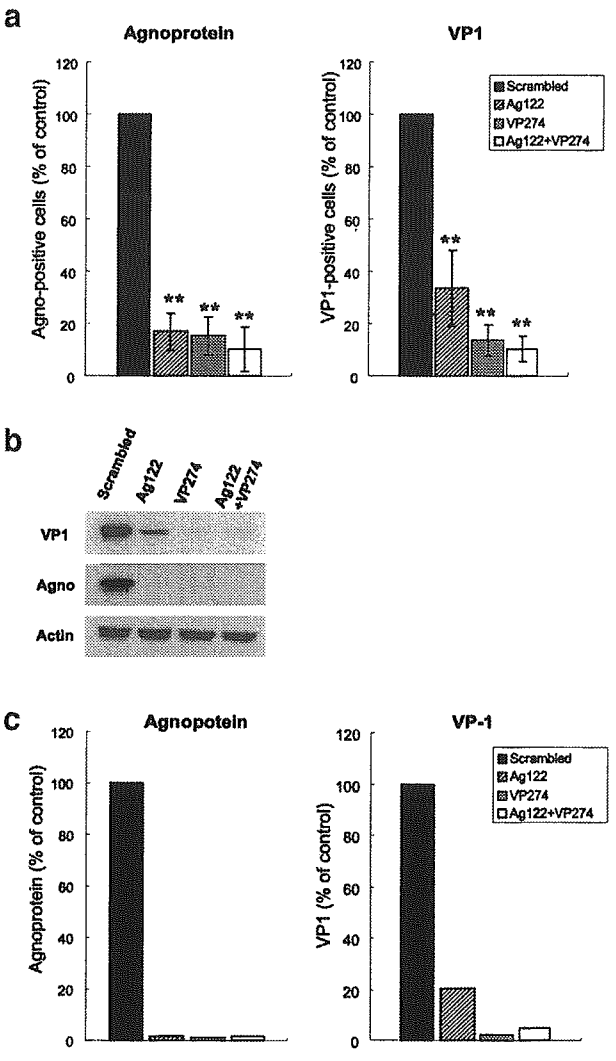

FIG. 2. Indirect immunofluorescence analysis of the effects of RNAi on viral protein expression in JCV-infected SVG-A cells. (a) The proportion of cells that were positive for agnoprotein or VP1 was determined by an indirect immunofluorescence analysis 48 h after transfection with the indicated siRNA(s). The data are expressed as percentages of the proportion determined for JCV-infected cells transfected with the scrambled siRNA (control) and are means ± standard deviations (SD) of values from at least three independent experiments. **, $P < 0.02$ versus the value for cells transfected with the scrambled siRNA (Student's t test). (b) Immunoblot analysis of VP1, agnoprotein, and actin expression in JCV-infected cells transfected with the indicated siRNA(s). (c) The signals for agnoprotein and VP1 were quantified with an image analyzer and expressed as percentages of the value for cells transfected with the scrambled siRNA.

after transfection with a siRNA, treated with DNase I, and subjected to RT with a Superscript first-strand synthesis system (Invitrogen) followed by real-time quantitative PCR with a GeneAmp5700 instrument (Applied Biosystems). The amount of each viral mRNA was normalized to that of β-actin mRNA in the same sample. The abundance of agnoprotein and VP1 mRNAs was significantly reduced in JCV-infected cells transfected with Ag122, VP274, or both siRNAs (Fig. 3). The reduction in the amounts of viral mRNAs, however, was not as large as that in the amounts of the encoded proteins. We eliminated the possibility of contamination of the viral DNA in the RT-PCR samples by (i) performing a DNase I treatment prior to RT-PCR, without the reverse transcriptase, and (ii) performing an RNase A treatment prior to the reverse transcriptase reaction. For both treatments, the RT-PCR signal was lost, suggesting that there was no contamination of the viral DNA in the RT-PCR samples. Whereas siRNAs are known to be incorporated into an RNA-induced silencing complex and to direct RNA-induced silencing complex-mediated sequence-specific mRNA degradation (9), the detailed mechanism of this process remains unclear. One possible explanation for the difference in the magnitude of the effects of the JCV-specific siRNAs on the amounts of viral RNAs and pro-

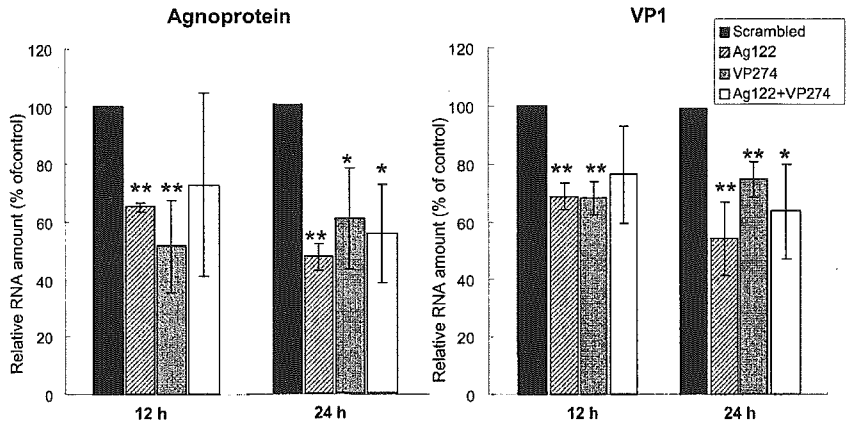

FIG. 3. Depletion of viral RNAs by RNAi in JCV-infected SVG-A cells. Total RNAs isolated from JCV-infected cells 12 or 24 h after transfection with the indicated siRNAs were subjected to an RT-PCR analysis of agnoprotein and VP1 mRNAs. The data were normalized to the amount of β-actin mRNA and are expressed as percentages of the normalized value for JCV-infected cells transfected with the scrambled siRNA (control); they are means ± SD of values from at least three independent experiments. *, $P < 0.05$, and **, $P < 0.02$ versus the value for cells transfected with the scrambled siRNA.

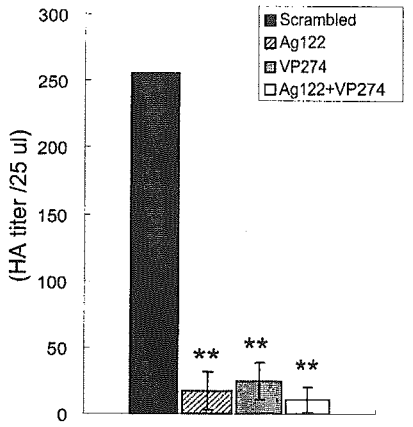

FIG. 4. Inhibition of JCV production by RNAi in SVG-A cells. Extracts prepared from JCV-infected cells 36 h after transfection with the indicated siRNAs were assayed for hemagglutination activity (HA). The data are expressed as HA titers per 25 μl of cell extract and are means ± SD of values from at least three independent experiments. **, $P < 0.02$ versus the value for cells transfected with the scrambled siRNA.

teins is that the target mRNA bound with a siRNA might be detected by RT-PCR before its degradation.

To examine the effect of RNAi on JCV production, we measured the hemagglutination activity (17, 22) of JCV-infected SVG-A cells 36 h after siRNA transfection. The hemagglutination activities of cells transfected with Ag122, VP274, or both of these siRNAs were 6.7, 9.3, and 4.1%, respectively, of that for cells transfected with the scrambled siRNA (Fig. 4). Thus, siRNAs that target agnoprotein or VP1 greatly inhibited JCV production in infected cells.

In summary, we have achieved a marked inhibition of JCV production by RNAi in cells already infected with the virus. Our results may have important implications for the development of a new approach to the treatment of PML. The application of an RNAi-based antiviral strategy for PML will require an efficient and specific delivery of siRNAs to the central nervous system.

We thank Mayumi Sasada for technical assistance.

This study was supported in part by grants from the Ministry of Education, Science, Sports, and Culture and by grants from the Ministry of Health, Labour and Welfare, Japan.

REFERENCES

1. **Andino, R.** 2003. RNAi puts a lid on virus replication. Nat. Biotechnol. **21**:629–630.
2. **Clifford, D. B.** 1999. Opportunistic viral infections in the setting of human immunodeficiency virus. Semin. Neurol. **19**:185–192.
3. **Endo, S., Y. Okada, Y. Orba, H. Nishihara, S. Tanaka, K. Nagashima, and H. Sawa.** 2003. JC virus agnoprotein colocalizes with tubulin. J. Neurovirol. **9**(Suppl. 1):10–14.
4. **Frisque, R. J., G. L. Bream, and M. T. Cannella.** 1984. Human polyomavirus JC virus genome. J. Virol. **51**:458–469.
5. **Ge, Q., M. T. McManus, T. Nguyen, C. H. Shen, P. A. Sharp, H. N. Eisen, and J. Chen.** 2003. RNA interference of influenza virus production by directly targeting mRNA for degradation and indirectly inhibiting all viral RNA transcription. Proc. Natl. Acad. Sci. USA **100**:2718–2723.
6. **Gitlin, L., S. Karelsky, and R. Andino.** 2002. Short interfering RNA confers intracellular antiviral immunity in human cells. Nature **418**:430–434.
7. **Giudici, B., B. Vaz, S. Bossolasco, S. Casari, A. M. Brambilla, W. Luke, A. Lazzarin, T. Weber, and P. Cinque.** 2000. Highly active antiretroviral therapy and progressive multifocal leukoencephalopathy: effects on cerebrospinal fluid markers of JC virus replication and immune response. Clin. Infect. Dis. **30**:95–99.
8. **Hall, C. D., U. Dafni, D. Simpson, D. Clifford, P. E. Wetherill, B. Cohen, J. McArthur, H. Hollander, C. Yainnoutsos, E. Major, L. Millar, and J. Timpone.** 1998. Failure of cytarabine in progressive multifocal leukoencephalopathy associated with human immunodeficiency virus infection. AIDS Clinical Trials Group 243 Team. N. Engl. J. Med. **338**:1345–1351.
9. **Hammond, S. M., E. Bernstein, D. Beach, and G. J. Hannon.** 2000. An RNA-directed nuclease mediates post-transcriptional gene silencing in *Drosophila* cells. Nature **404**:293–296.
10. **Jacque, J. M., K. Triques, and M. Stevenson.** 2002. Modulation of HIV-1 replication by RNA interference. Nature **418**:435–438.
11. **Kerr, D. A., C. F. Chang, J. Gordon, M. A. Bjornsti, and K. Khalili.** 1993. Inhibition of human neurotropic virus (JCV) DNA replication in glial cells by camptothecin. Virology **196**:612–618.
12. **Komagome, R., H. Sawa, T. Suzuki, Y. Suzuki, S. Tanaka, W. J. Atwood, and K. Nagashima.** 2002. Oligosaccharides as receptors for JC virus. J. Virol. **76**:12992–13000.
13. **Liu, C. K., G. Wei, and W. J. Atwood.** 1998. Infection of glial cells by the human polyomavirus JC is mediated by an N-linked glycoprotein containing terminal α(2–6)-linked sialic acids. J. Virol. **72**:4643–4649.
14. **Lynch, K. J., and R. J. Frisque.** 1991. Factors contributing to the restricted DNA replicating activity of JC virus. Virology **180**:306–317.
15. **Marra, C. M., N. Rajicic, D. E. Barker, B. A. Cohen, D. Clifford, M. J. Donovan Post, A. Ruiz, B. C. Bowen, M. L. Huang, J. Queen-Baker, J. Andersen, S. Kelly, and S. Shriver.** 2002. A pilot study of cidofovir for progressive multifocal leukoencephalopathy in AIDS. AIDS **16**:1791–1797.
16. **Novina, C. D., M. F. Murray, D. M. Dykxhoorn, P. J. Beresford, J. Riess, S. K. Lee, R. G. Collman, J. Lieberman, P. Shankar, and P. A. Sharp.** 2002. siRNA-directed inhibition of HIV-1 infection. Nat. Med. **8**:681–686.
17. **Nukuzuma, S., Y. Yogo, J. Guo, C. Nukuzuma, S. Itoh, T. Shinohara, and K. Nagashima.** 1995. Establishment and characterization of a carrier cell culture producing high titres of polyoma JC virus. J. Med. Virol. **47**:370–377.
18. **Okada, Y., S. Endo, H. Takahashi, H. Sawa, T. Umemura, and K. Nagashima.** 2001. Distribution and function of JCV agnoprotein. J. Neurovirol. **7**:302–306.
19. **Okada, Y., H. Sawa, S. Endo, Y. Orba, T. Umemura, H. Nishihara, A. C. Stan, S. Tanaka, H. Takahashi, and K. Nagashima.** 2002. Expression of JC virus agnoprotein in progressive multifocal leukoencephalopathy brain. Acta Neuropathol. (Berlin) **104**:130–136.
20. **Safak, M., R. Barrucco, A. Darbinyan, Y. Okada, K. Nagashima, and K. Khalili.** 2001. Interaction of JC virus agno protein with T antigen modulates transcription and replication of the viral genome in glial cells. J. Virol. **75**:1476–1486.
21. **Shishido-Hara, Y., Y. Hara, T. Larson, K. Yasui, K. Nagashima, and G. L. Stoner.** 2000. Analysis of capsid formation of human polyomavirus JC (Tokyo-1 strain) by a eukaryotic expression system: splicing of late RNAs, translation and nuclear transport of major capsid protein VP1, and capsid assembly. J. Virol. **74**:1840–1853.
22. **Suzuki, S., H. Sawa, R. Komagome, Y. Orba, M. Yamada, Y. Okada, Y. Ishida, H. Nishihara, S. Tanaka, and K. Nagashima.** 2001. Broad distribution of the JC virus receptor contrasts with a marked cellular restriction of virus replication. Virology **286**:100–112.
23. **Weber, T., and E. O. Major.** 1997. Progressive multifocal leukoencephalopathy: molecular biology, pathogenesis and clinical impact. Intervirology **40**: 98–111.